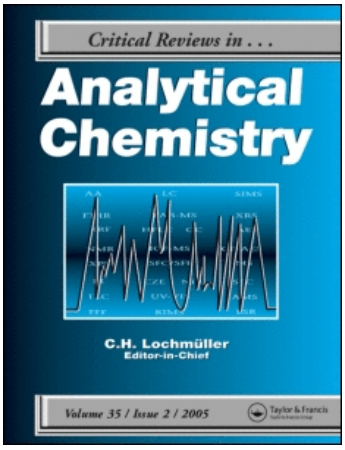

Critical Reviews in Analytical Chemistry
Publication details, including instructions for authors and subscription information:
http://www.informaworld.com/smpp/title~content=t713400837

A Critical Comparison of Atomic Emission, Atomic Absorption, and Atomic Fluorescence Flame Spectrometry

J. D. Winefordner; V. Svoboda; L. J. Cline; V. A. Fassel

To cite this Article Winefordner, J. D. , Svoboda, V. , Cline, L. J. and Fassel, V. A.(1970) 'A Critical Comparison of Atomic Emission, Atomic Absorption, and Atomic Fluorescence Flame Spectrometry', Critical Reviews in Analytical Chemistry, 1: 2, 233 — 272
To link to this Article: DOI: 10.1080/10408347008542736
URL: http://dx.doi.org/10.1080/10408347008542736

A CRITICAL COMPARISON OF ATOMIC EMISSION, ATOMIC ABSORPTION, AND ATOMIC FLUORESCENCE FLAME SPECTROMETRY

Authors: **J.D. Winefordner.* V. Svoboda, and L.J. Cline**
Department of Chemistry
University of Florida
Gainesville, Florida

Referee: V.A. Fassel
Ames Laboratory USAEC
Iowa State University
Ames, Iowa

TABLE OF CONTENTS

* This work was supported by AFOSR (SRC)-OAR, U.S.A.F. Grant No. AF-AFOSR-70-1880.

I. INTRODUCTION

In all flame spectrometric methods, a sample solution (containing the analyte) is nebulized by means of a chamber external to the flame or by means of the flame to produce an aerosol. Within the flame, solvent evaporates from the resulting aerosol to produce solute particles which then undergo vaporization to produce molecules of the various components of the sample matrix. The only molecules of analytical interest are those that contain the analyte atom; these molecules must undergo dissociation to produce analyte atoms for measurement by atomic emission (AE), atomic absorption (AA), or atomic fluorescence (AF) flame spectrometry. Other equilibrium processes, such as ionization of analyte atoms and compound formation of the analyte atoms with flame gas products, compete with the dissociation process in the production of a population of analyte atoms. Of course, the kinetic processes of solvent and solute vaporization also limit the population of analyte atoms in the flame gases. *Because analyte atoms in the flame gases are essential to AE, AA, and AF, any kinetic or equilibrium process influencing the concentration of analyte atoms in the flame gases will affect each method in exactly the same manner, assuming the same flame is used in each method.*

Atomic emission (AE), atomic absorption (AA), and atomic fluorescence (AF) flame spectrometry, therefore, differ only in the mechanism of excitation and the means of measurement of characteristic signals. In AA, the analyte atoms are excited by means of an external light source and the fraction of radiation absorbed as a result of radiational excitation is measured. In AF, the analyte atoms are again radiationally excited as in AA, but the measured parameter is now a portion of the atomic fluorescence radiation resulting when a fraction of the excited atoms undergo radiational deactivation. In AE, the analyte atoms are excited via collisional means with flame gas molecules* and a portion of the radiation emitted when a fraction of the excited atoms undergoes radiational deactivation is measured. The basic instrumental systems and processes are shown in Figure 1.

In this manuscript, the similarities and differences among AE, AA and AF will be critically discussed, particularly with respect to the relative signals and signal-to-noise ratios, the shapes of analytical curves, the limits of detection, the presence of interferences, and the instrumentation. In the theoretical comparisons to be made, AE will be chosen as the reference technique. On the other hand, for most experimental comparisons the reference technique will be AA because this is the flame method currently most used for trace metal analysis.

The authors of this manuscript wish to point out that much of the theoretical approach to, expressions for, and discussion of line radiances and the shapes of radiance vs. atomic concentration curves is a direct result of the many excellent papers, chapter, and talks given by Professor C. Th. J. Alkemade and his coworkers at Utrecht. Analytical chemists are indeed fortunate to have such a fine group of physicists interested in the fundamental aspects of analytical flame spectrometry. The authors would also like to stress that the general idea of a comparison of flame methods is not new. Professor V.A. Fassel of Iowa State University has presented during the past three years on three different continents 36 invited lectures on a critical experimental comparison of the analytical capabilities of flame emission and atomic absorption spectrometry. We are truly indebted to Professor Fassel for exciting in us the desire to write this rather extensive theoretical and experimental comparison of flame methods.

II. LINE RADIANCES IN AE, AA, AND AF (1-3)

A. Thermodynamic Equilibrium in Flames

A thorough and detailed discussion of thermodynamic equilibrium, the rate at which it is attained, and deviations from it are given by Alkemade and Zeegers.[4] The following discussion is taken in part from the above authors.

* Atoms may also be excited *via* chemical reactions, in which case the process is called chemiluminescence.

Flame equilibrium is achieved if the flame temperature is the same at all points in the flame body and if all forms of energy are equilibrated among each other (the principle of detailed balance which is based upon the principle of microscopic reversibility strictly holds).

Local differences in temperature occur even in pre-mixed laminar flames because the flame is not truly an adiabatic system. In addition, the supply of fuel and oxidant is not completely homogeneous because of the radiation of heat to the environment, secondary combustion at the flame boundaries, and convection. Therefore, net transfer of heat, radiation, and mass occurs throughout the flame, so, strictly, there can be no thermodynamic equilibrium. However, as long as the rates of transport of heat, radiation, and mass are small compared with the rate of equipartitioning of energy over the different forms, it is still possible to talk of a local thermodynamic equilibrium characterized by a local temperature. In all subsequent discussion, it is assumed that the "local" region of the flame in question is in thermodynamic equilibrium.

The equilibration of flame energy at a given point over the various translational and internal degrees of freedom and for molecular dissociation and atomic ionization processes requires an exchange of energy by means of collisions with the surrounding molecules in a time interval of about 1 millisecond. Because the velocity of the flame gases is of the order of 1–10 m sec^{-1}, a molecule in the flame gases undergoes about 10^6 collisions with flame gas molecules while traveling above the reaction zone to the portion of the flame which is within the viewing field of the spectrometer.

FIGURE 1

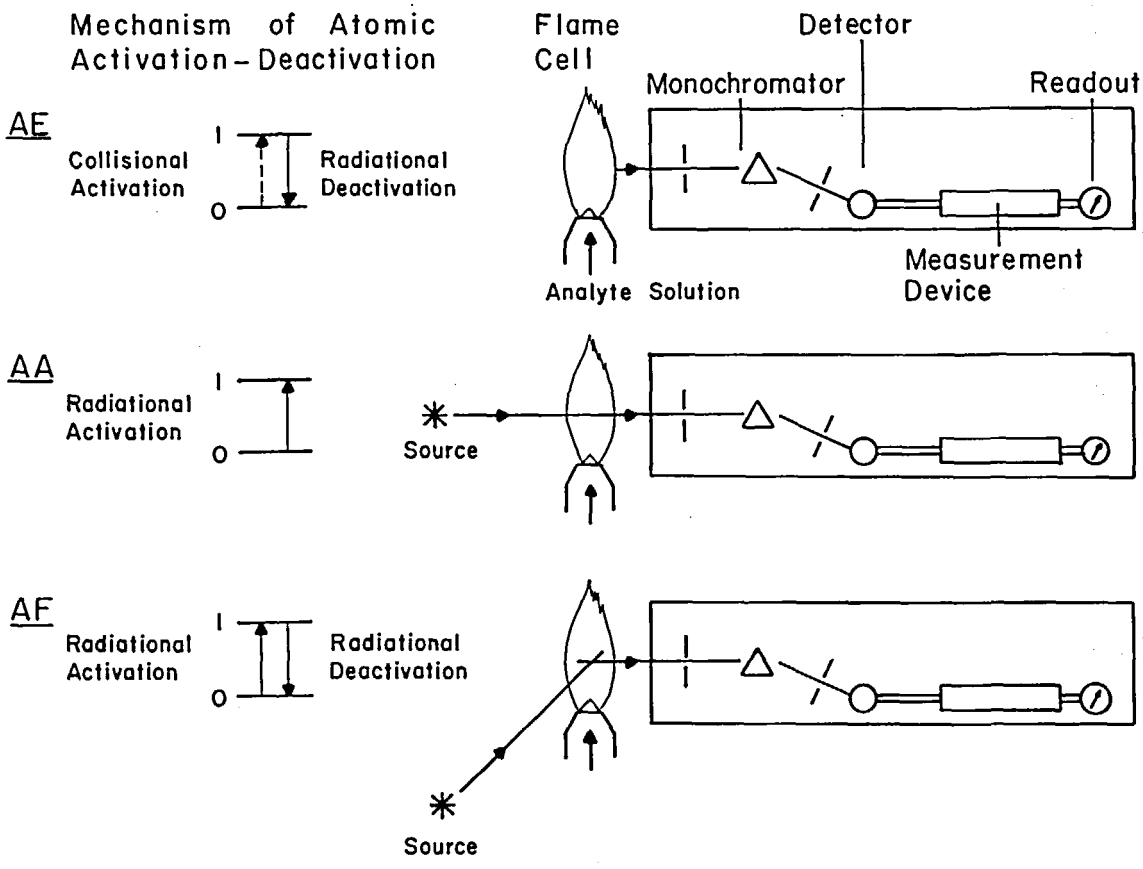

Basic Instrumental Systems for Atomic Emission (AE), Atomic Absorption (AA), and Atomic Fluorescence (AF) Flame Spectrometry.

Because the establishment of a Maxwell equilibrium distribution for the translational and rotational energies of flame gas molecules requires only 1–10 collisions, equilibrium among these degrees of freedom will be established almost immediately. The equipartition of energy over the vibrational degrees of freedom of flame molecules is a slower process and requires about 10^2 collisions. Because of the presence of large concentrations of CO_2 and H_2O molecules in most flames and because these molecules have short relaxation times, approximate vibrational equilibrium also exists. This is significant because of the importance of vibrational energy transfer in excitation of electronic states of atoms in AE.

The equilibration of energy over electronic states of flame molecules requires about 10^4 collisions per molecule and so may not be achieved during the 1 millisecond time period. Suprathermal OH radiation has been observed for some milliseconds above the reaction zones of shielded pre-mixed laminar flames. Even though electronic excitation energy is *not* expected to be important in the excitation of atoms in AE,[1] thermodynamic equilibrium with respect to electronic excitation can be considered to hold approximately for regions above the reaction zone.

The establishment of thermodynamic equilibrium with respect to molecular dissociation requires about 10^4 collisions and also may not be achieved during the 1 millisecond time. The general agreement of calculated and measured flame temperatures justifies the assumption that the major constituents in the flame gases (e.g., CO_2, O_2, H_2O, and H_2 among others) are present in their equilibrium concentrations above the reaction zone. This comment does *not* hold for the radicals (such as H, O, and OH) formed in excess in the reaction zone, because of the rather slow recombination of these radicals to form stable molecules by ternary collision processes.[4]

The existence of thermodynamic equilibrium with respect to ionization is also questionable (about 10^6 collisions per molecule required) particularly in the reaction zone of hydrocarbon flames which contain an excess of positive and negative ions. The concentrations of the natural flame ions present in excess decay rather slowly with height above the reaction zone and so exceed their equilibrium values. This can also cause a height-dependent analyte ionization. Because ionization is unimportant in the excitation—de-excitation of analyte atoms, small deviations from ionization equilibrium within the flame gases should not affect the assumption of thermodynamic equilibrium.

If thermodynamic equilibrium exists, the distribution of energy over the various translational and internal degrees of freedom, the distribution of dissociation and ionization products, and spectral distribution of the radiation density are *governed by a single parameter, T, the temperature of the flame.* At a given T, these distributions depend only upon the temperature and the molecular properties of the individual species but *not* upon the type of interaction between them.[4,5] In analytical flames, thermodynamic equilibrium is approximated only over a small (local) region and this will be assumed here.

The five statistical distribution laws for the various forms of energy are the Maxwell Law for the velocity distribution of particles, the Boltzmann Law for the population of various discrete levels of internal energy of a particle, the mass action law relating concentration of reaction products to those of reactants at equilibrium, the Saha Law relating the concentrations of neutral species to those of the corresponding ionic species and free electrons, and the Planck Law of radiation for a black-body.

The fraction of particles with mass m having a kinetic energy equal to E_k within a spread dE_k is given[4] by the Maxwell Law

$$f(E_k)\,dE_k = \frac{2}{\sqrt{\pi}}\sqrt{\frac{E_k}{(kT)^3}}\,\exp(-E_k/kT)\,dE_k \qquad (1)$$

where k is the Boltzmann constant.

The ratio of the population of the uth level, n_u, to the total population n_t in all levels is given[4] by the Boltzmann Law

$$\frac{n_u}{n_t} = \frac{g_u \exp(-E_u/kT)}{\sum_i g_i \exp(-E_i/kT)} \qquad (2)$$

where the gs are the statistical weights of the various levels designated by subscripts, E_u is

the excitation energy of the uth level, and the summation is the electronic partition function. The Boltzmann Law describes the relative populations of the electronic, vibrational, and rotational states. The statistical weight factors of electronic states depend upon the total orbital and spin angular momenta or upon the total angular momentum of the levels involved. The statistical weight factor is unity for the vibrational levels of a diatomic molecule (diatomic molecules are of greatest analytical interest) and is dependent upon the rotational quantum number for the rotational levels.

The mass action law for the equilibrium

$$AB \rightleftarrows A + B \tag{3}$$

is given by

$$\underline{K}_{\underline{d}}(\underline{T}) = \frac{(\underline{n}_A)(\underline{n}_B)}{\underline{n}_{AB}} \tag{4}$$

where the ns are concentrations of the respective species (in number of species cm^{-3}) and $K_d(T)$ is the equilibrium constant for dissociation which depends upon the temperature T.

The Saha Law for the ionization equilibrium

$$A \rightleftarrows A^+ + \underline{e} \tag{5}$$

is given by

$$\underline{K}_{\underline{i}}(\underline{T}) = \frac{(\underline{n}_{A^+})(\underline{n}_{\underline{e}})}{\underline{n}_A} \tag{6}$$

where $K_i(T)$ is the temperature-dependent ionization equilibrium constant. The ionization constant $K_i(T)$ and the dissociation constant $K_d(T)$ can be calculated from well-known thermodynamic expressions.[4]

The spectral radiance $B_{B\lambda}$ of a black-body in thermodynamic equilibrium at temperature T is given by

$$\underline{B}_{B\lambda} = \underline{c}_1[\exp(\underline{hc}/\lambda\underline{kT})-1]^{-1} \tag{7}$$

where c_1 is a constant for any spectral line and is given by $c_1 = 8\pi hc^2\lambda^{-5}$, where c is the speed of light, h is the Planck constant, and λ is the wavelength of the line; k is the Boltzmann constant, and T is the temperature of the black-body. A black-body has by definition an absorption factor α_λ equal to unity at all wavelengths, i.e., it completely absorbs any radiation incident upon its surface. The absorption factor for a non-black-body α_λ is defined by Kirchhoff's Law:

$$\alpha_\lambda = \frac{\underline{B}_\lambda}{\underline{B}_{B\lambda}} \tag{8}$$

where B_λ is the spectral radiance of any radiating body with $\alpha_\lambda < 1$. For a black-body the emissivity ϵ_λ is the same as the absorption factor α_λ if the black-body is in thermodynamic equilibrium. Kirchhoff's Law holds exactly if the non-black-body is enclosed within a furnace at the same temperature as the body, and it even holds approximately for open flames where radiation equilibrium may not exist. The emission of radiation by a spectral line approaches the emission by a black-body only near the line center; and the value of α_λ indicates the degree to which the spectral line at any wavelength approximates that of a black-body. Kirchhoff's Law also holds for the emission coefficient e_λ, the emissivity per cm thickness of the radiating layer, and the absorption coefficient k_λ, the absorption factor per cm of absorbing (radiating) layer. The atomic absorption coefficient k_λ is an important atomic spectral parameter and is defined by the Voigt profile* expression

$$\underline{k}_\lambda = \frac{\underline{a}\kappa_0 \underline{n} f_{0u}}{\pi} \int_{-\infty}^{+\infty} \frac{\exp(-\underline{y}^2)d\underline{y}}{\underline{a}^2+(\underline{v}-\underline{y})^2} \tag{9}$$

where

$$\underline{v} = \frac{2\sqrt{\ln 2}\,(\lambda-\lambda_0)}{\Delta\lambda_D} \tag{10}$$

* The Voigt profile expression (Equation 9) accounts only for the combined effects of Gaussian (Doppler broadening) and Lorentzian (collisional and natural broadening) broadening but does not account for line shifts or asymmetry. The Voigt expression also applies only to a single isolated spectral line. If a line has hyperfine splitting and if each component is broadened by the Gaussian and Lorentzian components, then the Voigt profile expression can be applied to each component.[6,7]

$$a = \frac{\sqrt{\ln 2}\,\Delta\lambda_L}{\Delta\lambda_D} \tag{11}$$

$$\Delta\lambda_D = \frac{2\lambda_0}{c}\sqrt{\frac{2(\ln 2)\,KT}{M}} \tag{12}$$

$$\kappa_0 = \frac{2\sqrt{\ln 2}\,X\,\lambda_0^2}{\sqrt{\pi}\,c\,\Delta\lambda_D} \tag{13}$$

$$X = \frac{\pi e^2}{mc} \tag{14}$$

where λ is any wavelength in cm; λ_0 is the wavelength of the line center in cm; M is the atomic weight of the emitting or absorbing atom in g; f_{ou} is the absorption oscillator strength of the ground state (0) to upper state (u) transition and is dimensionless; m is the mass in g, and e the charge in esu of the electron; c is the speed of light in cm sec^{-1}; $\Delta\lambda_D$ is the Doppler half-width in cm; $\Delta\lambda_L$ is the Lorentzian (collisional) half-width in cm; a is the classical damping constant and is dimensionless; v is a variable dimensionless wavelength interval taken with respect to $\Delta\lambda_D$; and y is a dimensionless integration variable. It should be pointed out that $\kappa_0 n f_{ou}$ is generally replaced by k_0, which is the atomic absorption coefficient at λ_0 for pure Doppler broadening and is expressed in cm^{-1}, in most other references dealing with this subject; the substitution of $\kappa_0 n f_{ou}$ for k_0 is used in order to indicate the concentration-oscillator strength terms explicitly.

B. Derivation of Line Radiances

In order to compare theoretical limits of detection and analytical shapes in AE, AA, and AF, it is useful to derive expressions for the line radiances (in erg sec^{-1}cm^{-2}ster^{-1}) in these flame methods. The approach presented below follows the treatment given by Alkemade,[1] Hooymayers[2] and Zeegers, Smith, and Winefordner.[3] For the following discussion, it will be assumed that both the flame temperature T_F and the composition are constant throughout the region studied and that this region is in thermodynamic equilibrium for all three methods. It will also be assumed that the same resonance line, broadened primarily by Doppler and Lorentzian broadening, is measured in each method. The corresponding expressions for non-resonance lines will not be given here although they could be obtained by simple modification of the following treatment. In Figure 2, the geometries of the flame assumed in AE, AA, and AF are given.

1. *Atomic Emission Flame Spectrometry, AE*

Assuming the flame to be in thermodynamic equilibrium, the radiance B_{AE}, in erg sec^{-1}cm^{-2}-ster^{-1}, in AE is given[4,5,8,9] according to Kirchhoff's Law by

$$B_{AE} = B_{B\lambda_0} A_t \tag{15}$$

where $B_{B\lambda_0}$ is the spectral radiance (in erg sec^{-1}cm^{-2}ster^{-1}cm^{-1}) of a black-body at the flame temperature T_F and at the wavelength λ_0, and is given by the Planck Law [Equation 7]; and A_t is the total absorption and is defined by

$$A_t = \int \alpha_\lambda \, d\lambda \tag{16}$$

where α_λ is the absorption factor, which is wavelength dependent and is the fraction of radiation absorbed per unit wavelength interval.

For analytical flames having temperatures less than about 3500°K and wavelengths longer than about 2500 Å, $B_{B\lambda_0}$ is given by the Wien approximation of Equation 7

$$B_{B\lambda_0} = c_1 \exp(-hc/\lambda_0 kT_F) \tag{17}$$

where T_F is the flame temperature. It is assumed in Equation 15 that the black-body spectral radiance is essentially constant at all wavelengths extending for several times the line width in both directions from the line center. The $B_{B\lambda_0}$ factor in Equation 17 explains the extreme dependence of emission intensity upon flame temperature. On the other hand, the A_t factor, which is weakly dependent upon flame temperature, does describe the variation of *intensity* with ground state concentration n and flame depth l (the emission path length in the direction of the monochromator). Total

absorption is a function of the product nl and of the a-parameter which is defined as $\sqrt{ln2}\ (\Delta\lambda_L/\Delta\lambda_D)$, where $\Delta\lambda_L$ is the Lorentz half-intensity width and $\Delta\lambda_D$ is the Doppler half-intensity width of the emission (or absorption) line. However, A_t is dependent upon the a-parameter *only* if self-absorption is not negligible [if self-absorption is appreciable, so that $a > 0$, then $A_t = f_{un}\ (a)$]. The curve relating A_t (or some function proportional to A_t) to

FIGURE 2

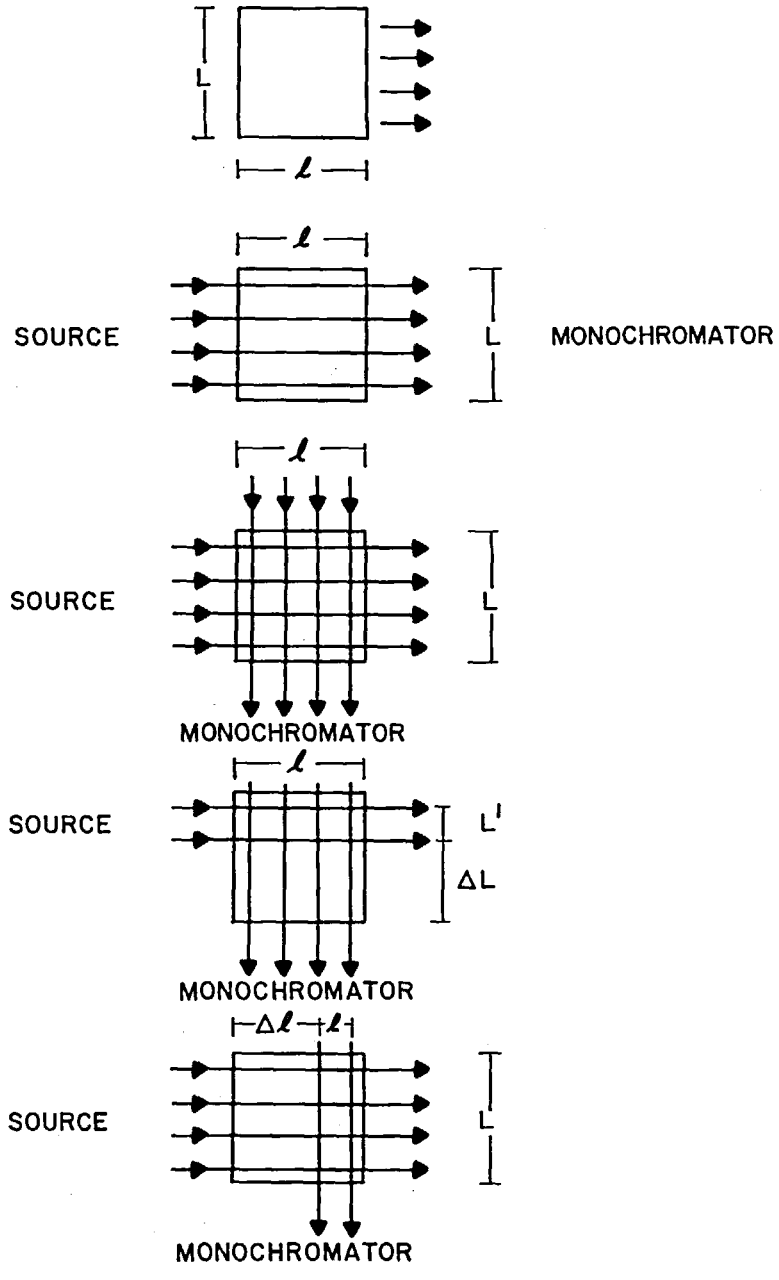

Schematic Diagram of Flame Cell Assumed for AE, AA and AF. It is assumed that the height of the illuminated region is ℓ' in each case. (1) AE; (2) AA; (3) AF assuming complete illumination and no inner filter effect; (4) AF assuming incomplete illumination and no inner filter effect; and (5) AF assuming complete illumination and inner filter effect.

FIGURE 3

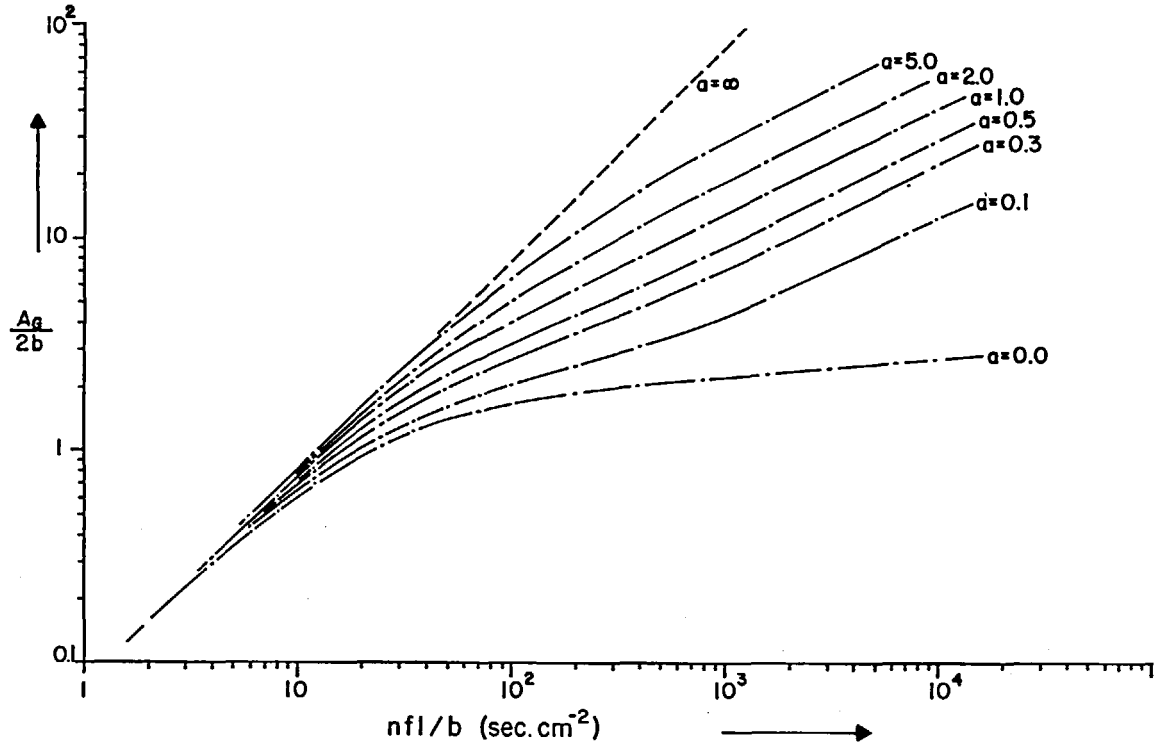

Theoretical Growth Curves for a Single Spectral Line for Various Values of the a-Parameter ($b = \pi c\, \Delta\lambda_D/\lambda_0^2\sqrt{\ln 2}$.

nl (or some function proportional to *nl*) is called the *curve of growth*. The integral absorption is given[6] by

$$\underline{A_t} = \int_0^\infty [1-\exp(-\underline{k_\lambda}\,\underline{\ell})]\,d\lambda \qquad (18)$$

where all terms have been previously defined.

In Figure 3, several growth (log-log) plots[7-10] for different a-parameter values are given. For small optical densities (i.e., small values of nl) all curves approach a linear asymptote $A_t \propto$ nl, and for large optical densities (i.e., large values of nl) all curves approach a square root asymptote $A_t \propto \sqrt{nl}$ as long as $a > 0$. The square-root asymptote is due to the *self-absorption phenomenon.** The values of A_t in the low-optical-density region are given by

$$\underline{A_t} = \int_0^\infty [1-\exp(-\kappa_\lambda \ell)]\,d\lambda \cong \ell\int_0^\infty \underline{k_\lambda}\,d\lambda$$

$$= \frac{\sqrt{\pi}\,\kappa_0 \underline{nf\ell}\;\Delta\lambda_D}{2\sqrt{\pi \ln 2}} \qquad (19)$$

and in the high-optical-density region by

$$\underline{A_t} = \int_0^\infty [1-\exp(-\underline{k_\lambda}\,\ell)]\,d\lambda$$

$$\cong \sqrt{\frac{\sqrt{\pi}\,\kappa_0 \underline{nf\ell}\; a\;\Delta\lambda_D^2}{\ln 2}} \qquad (20)$$

It should be noted from Figure 3 that the growth curves show an inflection if $0 < a \lesssim 1$.

* It should be noted that self-reversal is a phenomenon occurring only when there is a temperature gradient in an emitting source. Self-absorption, on the other hand, occurs when the flame gases have the same temperature at all points.

Also note that the slope is less than ½ at some intermediate value of nl[1] for curves with $\lesssim 1$.

2. *Atomic Absorption Flame Spectrometry, AA*

The spectral radiance $B_{A\lambda}$ (in erg $sec^{-1}cm^{-2}ster^{-1}cm^{-1}$) absorbed at wavelength λ from a source with a spectral radiance $B_{S\lambda}$ (also in erg $sec^{-1}cm^{-2}ster^{-1}cm^{-1}$) by an atomic vapor with a spectral absorption coefficient k_λ is given by

$$B_{A\lambda} = B_{S\lambda}[1-\exp(-k_\lambda \ell)] \quad (21)$$

The total radiance absorbed B_{AA} (in erg $sec^{-1}cm^{-2}ster^{-1}$) is given[11,12] by

$$B_{AA} = \int B_{A\lambda}\, d\lambda = \int B_{S\lambda}[1-\exp(-k_\lambda \ell)]d\lambda \quad (22)$$

where all terms have been defined above. It should be noted that $B_{S\lambda}$ is analogous to $B_{B\lambda}$ in AE. The integration limits depend upon the absorption line width and source characteristics.

In AA there are two possible means of excitation of the analyte atomic vapor. One can use either a *continuum* source-monochromator system with a spectral bandwidth *s* greater than the absorption line half-width $\Delta\lambda_A$ or a *line* source-monochromator system with a source line half-width $\Delta\lambda_S$ smaller than the absorption line half-width $\Delta\lambda_A$. The two cases will be designated as atomic absorption with a continuum source (AAC) and atomic absorption with a line source (AAL). If a continuum source-monochromator system is used in AA, the integration in Equation 22 is over the "entire" absorption line and $B_{S\lambda}$ is assumed to be constant. If a narrow line source is used, the integration in Equation 22 is only over the source line width.

If a *continuum source* is used, then

$$B_{AAC} = B_{C\lambda_0} A_t \quad (23)$$

where $B_{C\lambda_0}$ is the spectral radiance of the continuum source over the absorption line half-width $\Delta\lambda_A$. The great similarity between Equations 15 and 23 should be noted. The concentration dependence of the line radiance in AAC should be identical to that in AE because both depend linearly upon the integral absorption A_t (see discussion following equation 20). In addition, $B_{C\lambda_0}$ can be given by an expression identical with equation 17 [or 7] except that T_F must be replaced by the effective black-body temperature T_S of the source.

If a *line source* is used in AA,[11,12] then

$$B_{AAL} = [1-\exp(-k_m \ell)]B_L \quad (24)$$

where k_m is the average atomic absorption coefficient at the absorption line peak and B_L is the radiance (in erg $sec^{-1}cm^{-2}ster^{-1}$) of the line source, ie., $B_L = \int_{\Delta\lambda_S} B_{L\lambda}\, d\lambda$. For low concentrations of antlyte (i.e., low optical densities or small values of $k_m l$)

$$B_{AAL} \cong k_m \ell B_L \quad (25)$$

while for high concentrations of antlyte

$$B_{AAL} \cong B_L \quad (26)$$

In the latter case all of the radiation of the entire source line is absorbed (i.e., the flame is essentially opaque to the source resonance line at very high optical densities). The value of k_m for a source with $\Delta\lambda_S \lesssim \Delta\lambda_A$ is given[11] by

$$k_m = \kappa_0 nf\delta_0 \quad (27)$$

where δ_0 is simply the ratio $k_\lambda/\kappa_0 nf$ given by Equation 9.* Tables are available[10,13-15] for the evaluation of δ_0. Of course κ_0 is independent of *nf*, and δ_0 is approximately independent of *nf* and dependent primarily upon the flame gas temperature and composition and the spectral characteristics of the analyte atoms.

The measured parameter in AAC or AAL is seldom radiance (B_{AAC} or B_{AAL}) but, rather, is the fraction of radiance absorbed α (or the absorbance A) which is given for a continuum source by

* The parameter δ_0 is evaluated for the a-parameter corresponding to the absorption line of the analyte atom in the desired flame and for a v-value which is approximately given by $\Delta\lambda_S/\Delta\lambda_A$, i.e., the absorption coefficient for this v-value is an average over the source line width, $\Delta\lambda_S$.

$$\alpha_{AAC} = \frac{B_{AAC}}{\int \underline{B}_{C\lambda} d\lambda} = \frac{B_{AAC}}{s\ \underline{B}_{C\lambda_0}} \qquad (28)$$

where s is the spectral bandwidth of the monochromator; for a line source it is given by

$$\alpha_{AAL} = \frac{B_{AAL}}{\int \underline{B}_{L\lambda} d\lambda} = \frac{B_{AAL}}{\underline{B}_L} \qquad (29)$$

The absorbance is defined by $A = -\log(1-\alpha)$.

3. *Atomic Fluorescence Flame Spectrometry, AF*

In AF, there are two possible ways of exciting the analyte atomic vapor.[2,16,17] A *continuum* source (with or without an excitation monochromator) and a *line* source (with or without an excitation monochromator) can be used. The former case will be designated as AFC and the latter as AFL. In AFC it will be assumed that the source half-width $\Delta\lambda_S$ (or the spectral bandwidth s of the excitation monochromator if one is used) is much greater than the absorption line half-width $\Delta\lambda_A$, and in AFL it will be assumed that $\Delta\lambda_S < \Delta\lambda_A$.

For AF, we will assume an illuminated brick-shaped flame [see Figure 2-(3)] having path lengths of l cm in the direction of the excitation beam and of L cm in the direction of the emission monochromator, and l' cm high. It will be assumed that corrections have been made for any thermal emission at or near λ_0. The line radiance in AF is therefore given by

$$\underline{B}_{AF} = \left(\frac{\Omega_A}{4\pi}\right) \underline{B}_{AA} \left(\frac{\underline{L}}{\underline{l}}\right) \underline{Y} \left[\frac{\underline{A}_t(n\underline{L})}{\int_0^\infty \underline{k}_\lambda \underline{L} d\lambda}\right] \qquad (30)$$

where B_{AA} is given for AAC and AAL by use of the expressions in Section IIB2 above; the factor $\Omega_A/4\pi$ is the fractional solid angle of radiation collected from the source and impinging upon the flame, assuming the entire area $L \times l'$ to be illuminated as in Figure 2-(3), $L \times l$ accounts for the flame area excited and the flame area fluorescing in the direction of the emission monochromator, Y is the quantum yield for the resonance fluorescence, and the final term accounts for reabsorption of the fluorescence by ground state analyte atoms in the direction of the emission monochromator. The final term is simply the fraction of fluorescence radiation absorbed in the emission path length L and for low optical densities (low nL) is given[2] by

$$\frac{\underline{A}_t(n\underline{L})}{\int_0^\infty \underline{k}_\lambda \underline{L} d\lambda} = \frac{\int_0^\infty [1-\exp(-\underline{k}_\lambda L)] d\lambda}{\int_0^\infty \underline{k}_\lambda \underline{L} d\lambda}$$

$$\underline{\simeq} \frac{\int_0^\infty \underline{k}_\lambda \underline{L} d\lambda}{\int_0^\infty \underline{k}_\lambda \underline{L} d\lambda} = 1 \qquad (31)$$

and for high optical densities (high nL) is given[2] by

$$\frac{\underline{A}_t(n\underline{L})}{\int_0^\infty \underline{k}_\lambda \underline{L} d\lambda} = \frac{\int_0^\infty [1-\exp(-\underline{k}_\lambda L)] d\lambda}{\int_0^\infty \underline{k}_\lambda \underline{L} d\lambda}$$

$$\underline{\simeq} \frac{\sqrt{\frac{\sqrt{\pi}\ \kappa_0 \underline{nf}\ \underline{La}\Delta\lambda_D^2}{\ln 2}}}{\frac{\sqrt{\pi}\ \kappa_0 \underline{nfL}\ \Delta\lambda_D}{2\sqrt{\ln 2}}} = \frac{2\sqrt{a}}{\sqrt{\sqrt{\pi}\ \kappa_0 \underline{nfL}}} \qquad (32)$$

The re-absorption factor is *not influenced by the means of excitation* but is dependent only upon the concentration and spectral characteristics of the analyte atoms and upon the path length L;[1] it is only slightly sensitive to flame temperature. The quantum yield is dependent not only upon the spectral characteristics of the analyte atoms but also upon the concentration and type of collisional quenching species (flame gas products) in the flame.[16,18-22]

In Equation 30 it is assumed that right angle illumination is used, that the entire flame width L is illuminated by the excitation beam, and that fluorescence over the entire flame width l is collected by the emission monochromator. However, if the flame cell is only partially illuminated, then the fluorescence radiance is necessarily reduced by re-absorption in the non-illuminated layer [see Figure 2-(4)]. If only the fluorescence from deep within the flame gases is observed, then an inner filter effect results [see Figure 2-(5)], and the fluorescence radiance is again reduced. Because incomplete illumination of the flame by the source radia-

tion [as in Figure 2-(4)] and measurement of only a portion of the fluorescence emitted towards the detector [as in Figure 2-(5)] are of less analytical use than complete illumination and measurement of all fluorescence emitted toward the detector [as in Figure 2-(3)], no expressions will be given for the former two cases [those depicted in Figures 2-(4) and 2-(5)]. Alkemade[1] and Hooymayers[2] have given equations for the fluorescence radiance for the cases depicted in Figures 2-(4) and 2-(5).

C. Expressions for Radiances

By combining the previous equations, expressions for the radiances for resonance lines in AE, AAC, AAL, AFC, and AFL are obtained for the low- and high-concentration regions (see Table I for expressions for the radiance B in AE, AAC, AAL, AFC, and AFL, and for α in AAC and AAL). For the case of AFC and AFL, right-angle illumination as shown in Figure 2-(3) is assumed. Also, all of the expressions are only valid for *low* and *high* concentrations and do not apply to the intermediate region.

The emission, absorption, and fluorescence radiances of resonance lines can be converted to instrumental signals by multiplying each radiance by an instrumental constant K, which converts radiance incident upon the monochromator entrance slit into photodetector signal

TABLE 1

Radiances in AE, AAC, AFC[a], and AFL.[a]

Method	Low Optical Density (Low $\underline{n\ell}$)[b]	High Optical Density (High $n\ell$)[b]
AE	$\underline{B}_{AE} = \underline{c}_2 \underline{B}_{B\lambda_0} \kappa_0 \underline{nf\ell}\ \Delta\lambda_D$	$\underline{B}_{AE} = \underline{B}_{B\lambda_0} \sqrt{\underline{c}_3 \kappa_0 \underline{nf\ell a}\ \Delta\lambda_D^2}$
AAC	$\underline{B}_{AAC} = \underline{c}_2 \underline{B}_{C\lambda_0} \kappa_0 \underline{nf\ell}\ \Delta\lambda_D$	$\underline{B}_{AAC} = \underline{B}_{C\lambda_0} \sqrt{\underline{c}_3 \kappa_0\ \underline{nf\ell a}\ \Delta\lambda_D^2}$
	$\alpha_{AAC} = \dfrac{\underline{c}_2 \kappa_0 \underline{nf\ell}\ \Delta\lambda_D}{\underline{s}}$	$\alpha_{AAC} = \dfrac{1}{\underline{s}} \sqrt{\underline{c}_3 \kappa_0 \underline{nf\ell a}\ \Delta\lambda_D^2}$
AAL	$\underline{B}_{AAL} = \underline{B}_L \kappa_0 \underline{nf\ell}\ \delta_0$	$\underline{B}_{AAL} = \underline{B}_L$
	$\alpha_{AAL} = \kappa_0 \underline{nf\ell}\ \ \delta_0$	$\alpha_{AAL} = 1$
AFC[a]	$\underline{B}_{AFC} = \underline{c}_2 \underline{B}_{C\lambda_0} \kappa_0 \underline{nfL}\ \Delta\lambda_D\ \underline{Y}\left(\dfrac{\Omega_A}{4\pi}\right)$	$\underline{B}_{AFC} = \dfrac{\underline{c}_3}{\underline{c}_2} \underline{B}_{C\lambda_0}\ \underline{a}\ \Delta\lambda_D \sqrt{\dfrac{\underline{L}}{\underline{\ell}}}\ \underline{Y}\left(\dfrac{\Omega_A}{4\pi}\right)$
AFL[a]	$\underline{B}_{AFL} = \underline{B}_L \kappa_0 \underline{nfL} \delta_0\ \underline{Y}\left(\dfrac{\Omega_A}{4\pi}\right)$	$\underline{B}_{AFL} = \underline{B}_L \sqrt{\dfrac{4\underline{a}\ \underline{L}}{\sqrt{\pi}\ \kappa_0\ \underline{nf\ell}^2}}\ \underline{Y}\left(\dfrac{\Omega_A}{4\pi}\right)$

a. For illumination as shown in Figure 2

b. $\underline{c}_2 = \sqrt{\pi}\ /2\sqrt{\ln 2}$

$\underline{c}_3 = \dfrac{\sqrt{\pi}}{\ln 2}$

$\kappa_0 = \underline{k}_0/\underline{nf}$

(if the source image is magnified in AA and AF, the K-factor must be divided by the magnification factor). Because the entire instrumental system for AE, AA, and AF is assumed to be identical except for the differences in entrance optics already mentioned, the instrumental constant K is therefore identical for all methods.

III. SHAPES OF THEORETICAL CURVES OF log B vs. log n

The shapes of theoretical curves of log B vs. log n can be obtained by using the expressions in Table I. For the cases of AFC and AFL the *method of illumination shown in Figure 2-(3)* is assumed. For any given atom, line, and flame the quantities $B_{B\lambda_0}$, a, Y, $\Delta\lambda_D$, L, l, and κ_0 are constant. For any given source $B_{C\lambda_0}$ and B_L are constants. For any given atom, line, flame, and line source δ_0 is a constant.[11] Of the above parameters (not considering the dependence of n on flame temperature T_F), only $B_{B\lambda_0}$ is critically dependent upon T_F. The a-parameter[23,24] and Y[16,18-22] depend less critically upon flame temperature and flame gas composition. Typical growth curves for Mg in a typical analytical C_2H_2/air flame[3] are given in Figures 4 and 5.

A. log B_{AE} vs. log n [25,26]

The slope is 1.0 at low nl and 0.5 at high nl assuming a homogeneous flame in thermodynamic equilibrium.[27] The shape is identical with that of the growth curves of log A_t vs. log n given in Figure 3.

B. log B_{AAC} vs. log n [28-31]

The slope of the low- and high-concentration asymptotes are identical with those in AE. The only difference between the curves in AAC and AE is the absolute value of the ordinate for any given n-value; this is due to the differences between $B_{B\lambda_0}$ and $B_{C\lambda_0}$, which depend upon T_F and T_S, respectively. It is interesting to note that the curve of log B_{AAC} vs. log n is independent of s, the spectral bandwidth of the monochromator. However, it is generally α, the fraction absorbed, that is measured, and the curve log α vs. log n does shift and change shape when s is increased.[11,12]* Plots of the absorbance A vs. log n also shift and change form with variation in s.

C. log B_{AAL} vs. log n

The slope is 1.0 at low nl-values and —0.0 and the slope of the high-nl asymptote is zero (i.e., when nl is high the flame becomes opaque and $B_{AAL} \rightarrow B_L$ while $\alpha \rightarrow 1.0$). It is interesting to note that conventional line sources should result in greater α-values (and greater B_{AAL}-values) than continuum sources with monochromators having spectral bandwidths[11] where our expressions are valid. However, the background noise with continuum sources should be lower[32] than with line sources, so that the limits of detection are comparable (see the following sections). It is surprising, therefore, that no commercial AA instrumentation utilizes continuum sources (see discussion of instrumentation).

D. log B_{AFC} vs. log n Assuming Illumination as in Figure 2-(3)

The slope is 1.0 at low nl-values and —0.0 at high nl-values. Therefore, analytical curves in AFC will have no analytical use at high concentrations of analyte. Of course, analyte solutions can be diluted to give values of nl that lie in the linear region of the curve.

E. log B_{AFL} vs. log n Assuming Illumination as in Figure 2-(3)

The slope is 1.0 at low nl-values and —0.5 for high nl-values. Again, solutions containing too high concentrations of analyte should be diluted for analysis.

F. log B_{AFC} or log B_{AFL} vs. log n Assuming Incomplete Illumination as in Figures 2-(4) and 2-(5)

If the flame cell is incompletely illuminated with exciting radiation as in Figure 2-(4), then

* The shapes of measured curves of log B_{AAC} vs. log n will actually approach those of log B_{AAL} vs. log n at high values of n when using a continuum source and monochromator with fixed spectral bandwidths. In AAC the measured B_{AAC} will approach a maximum value (i.e., α approaches unity) at high concentrations where the absorption line width exceeds s.

FIGURE 4

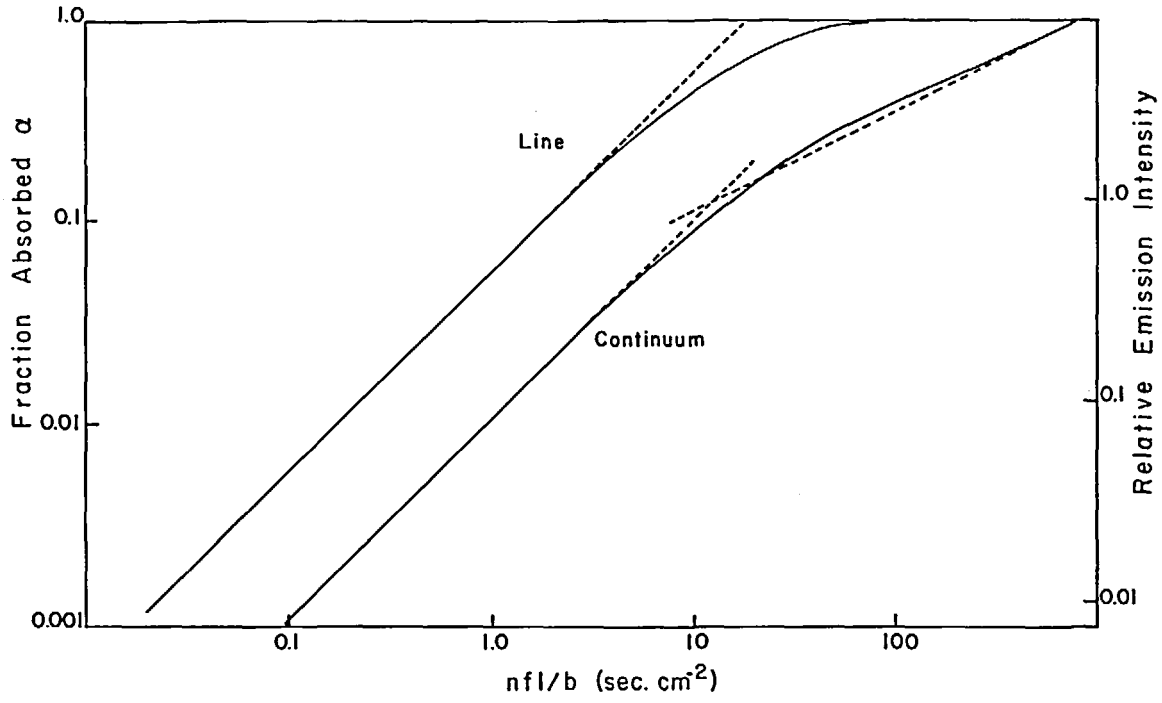

Growth curves for atomic absorption with a continuum source (atomic emission is represented by same curve, ordinate is of $B_{AE}\sqrt{\ln 2}/B_{E\lambda_0}\,\Delta\lambda_D$) with a narrow line source. Data used to calculate curves: $T_F = 2400°K$; $\lambda_0 = 2852$ Å (magnesium line); $\Delta\lambda_D = 0.0021$ nm; $a = 0.5$, $L = l = 1$ cm; $\Delta\lambda_S \leq 0.00025$ nm; $\delta_0 = 0.61$; and $s = 0.02$ nm.

FIGURE 5

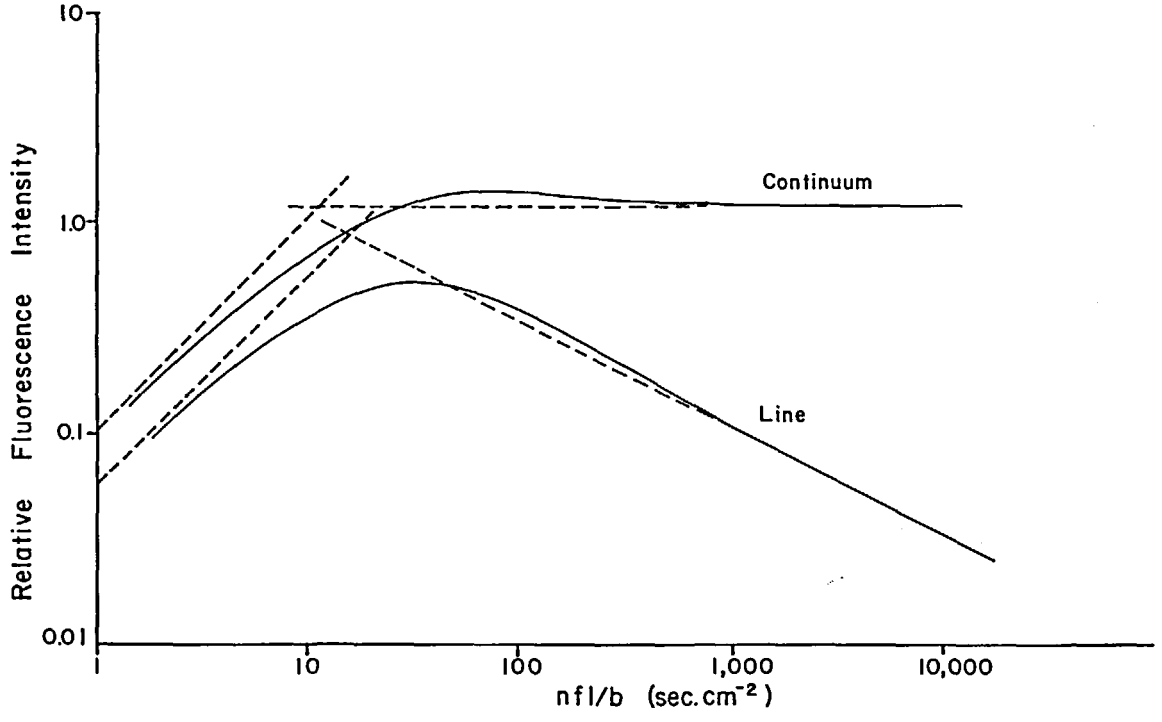

Growth curves for atomic fluorescence with a continuum source [ordinate $B_{AFC}/(\Omega_A/4\pi)YB_{C\lambda_0}\,\Delta\lambda_D$] and with a narrow line source [ordinate $B_{AFL}/(\Omega_A/4\pi)YB_{T_r}$]. Data used to calculate curves are in caption of Figure 4.

B_{AF} will be smaller than for complete illumination at high n. Partial measurement of the fluorescence as in Figure 2-(5) also causes B_{AF} to be smaller. P.TH.J. Zeegers[33] performed such measurements and verified the expressions given by Hooymayers[2] for the cases of incomplete illumination.

IV. SHAPES OF ANALYTICAL CURVES

A. Relationship between Concentrations of Analyte in Flame (n) and in Solution (C)

The log B vs. log n curves determine the shapes of analytical curves, which are plots of log S vs. log C, where S is the photodetector signal and C is the concentration of the analyte in the solution. The signal S should be directly proportional to B over the entire range of analytically useful concentrations.[34-37] However, n may not be linear with C at all values of C, because of variations of the degree of ionization, solute vaporization, aspirator yield, and solution-transport rate with C.[3] The relationship between n (number of analyte atoms in ground state cm^{-3}) and C (moles of analyte cm^{-3}) is given[1 3 4] by

$$n = 6 \times 10^{23}\left(\frac{F\epsilon\beta C}{Qe_f B(T)}\right) \qquad (34)$$

where F is the transport rate of solution as determined by the nebulizer ($cm^3\ sec^{-1}$), ϵ is the efficiency of producing analyte molecules in the flame[38] (dimensionless), β is the efficiency of atomization [free atom fraction[39]] (dimensionless), Q is the flow rate of unburnt gases into the flame ($cm^3\ sec^{-1}$), e_f is the flame gas expansion factor[8] (dimensionless), and $B(T)$ is the normalized partition function (dimensionless) $(1/g_o)\sum_i g_i \exp(-E_i/kT)$, where the g's are the statistical weights of the ground (0) and excited (i) states and E_i is the excitation energy of state i.

B. The Atomization Efficiency, β

The atomization efficiency β is the ratio of the concentration of free analyte atoms in the flame to the total concentration of analyte in all gaseous forms. This factor accounts for incomplete dissociation of the analyte compound introduced into the flame, for formation of compounds resulting between the analyte and flame gas molecules, and for ionization of the analyte atoms in the flame gases.

C. The Aspiration Efficiency, ϵ

The aspiration efficiency ϵ is the ratio of the number of all gaseous analyte species produced in the flame per unit time to the total number of analyte atoms aspirated per unit time. This factor accounts for vaporization of the solvent, volatilization of the solid particles in the flames, and also for the transfer efficiency (yield) of the aspirator chambers and associated tubes used with chamber type aspirator burners. Under analytical flame spectrometric conditions, many workers assume the constancy of ϵ and β at all values of the concentration of the analyte solution. It is well known, however, that large changes in n for a constant C can occur due to changes in ϵ and β resulting from changes in the solution matrix and/or changes in the flame gas composition and temperature.

D. Factors Affecting β

At low concentrations of analyte, β will vary with the analyte concentration C because of variation in the degree of ionization.[40] Zeegers, Smith, and Winefordner[3] derived an expression for β assuming that no compound formation occurs and that the metal M has M^+ as its only ionization form. If K_i, which is a function of T_F, is the ionization constant for the process $M \rightleftarrows M^+ + e$ (see Equation 5) and if electroneutrality [$n_e = n_{M^+} + n_f$, where n_f is the concentration of free electrons due to the flame gases and is assumed to be independent of n_T, and n_{M^+} is the concentration of electrons due to ionization of M] and material balance [$n_T = n_M + n_{M^+}$, where n_T is the total concentration of M in both the atomic and ionic forms] are valid, then

$$\beta = \frac{K_i + n_f}{2n_T} + 1 - \frac{1}{2}\sqrt{\frac{K_i^2 + 2n_f K_i + n_f^2 + 4K_i n_T}{n_T^2}} \qquad (35)$$

For non-hydrocarbon flames (for which $n_T \gg n_f$) and for low concentrations of M in all

forms (so that $K_1 \gg n_T$) β is given by

$$\beta = \frac{n_T}{K_1} \qquad (36)$$

and so the limiting slope of *all* analytical curves in flame spectrometry approaches a value of *2 instead of unity* as the concentration is made smaller. At high total M concentration in non-hydrocarbon flames ($n_T \gg K_1$ and $n_T \gg n_f$) or at most M concentrations in hydrocarbon flames ($n_f > n_T$)

$$\beta \cong 1 \qquad (37)$$

and so the analytical curve will have the same slope as the growth curve.

At high concentrations of flame gas products, the analyte M may form compounds with the flame gas products (O, OH, etc.). Assuming that the flame gas product is X, that no ionization of M occurs, that only the compound MX forms, and that its formation can be described by the equilibrium and dissociation constant K_d, which is a function of T_F (see Equations 3 and 4), it can be shown that

$$\beta = \frac{K_d}{K_d + n_X} \qquad (38)$$

where n_X is the concentration of flame gas products, X. Therefore, β is *independent of the total M concentration* n_T if $n_X > n_T$ (the usual case in flame spectrometry) and is *dependent only upon the flame gas composition and temperature and the particular compound formed.* Therefore compound formation *does not cause any change in shape* of analytical curves in AE, AA, or AF from the shapes of the log B vs. log n curves. Compound formation will vary with flame gas composition and temperature and will cause β to vary from flame to flame. On the other hand, incomplete dissociation of analyte molecules introduced into the flame is rare and should seldom cause β to vary from the value determined by Equation 38.

E. Factors Affecting ϵ

At high concentrations the aspiration efficiency ϵ can vary non-linearly with the analyte concentration.[3] In conventional flame methods of analysis the analyte is supplied to the flame in the form of an aerosol. Evaporation of the solvent may be complete before the analyte reaches the flame (as with some chamber-type aspirators) or may be incomplete even after the aerosol has passed through the flame (as with some total-consumption aspirator burners). The degree of solvent evaporation is fairly independent of the solute concentration and will have little effect on the shapes of the analytical curves that are obtained with a particular aspiration system. The subsequent evaporation of the residual solid or molten analyte particles, however, is a very critical step in flame analysis, for it affects both the position and shape of the analytical curves. The size distribution of the aerosol droplets produced by most chamber aspirators is independent of the concentration of analyte over a very wide range and, consequently, the dimensions of the particles remaining after evaporation of the solvent will be directly dependent on the droplet distribution and the solution concentration. If partial vaporization of the residual particles takes place, it is fairly obvious that the degree of vaporization will be lowest at high analyte concentrations, i.e., ϵ will decrease as the analyte concentration increases.

At the present time, it is impossible to predict accurately the variation of ϵ with C. However, the basic theory necessary for calculation has been derived by scientists interested in the evaporation of aerosols.[41-49] For example, the evaporation-rate equations of Fuchs[43] modified by Okuyama and Zung[44] could possibly describe the rate of solute vaporization in flames if the *evaporation process is diffusion-controlled.* For larger particles, which do not move with the rise velocity of the flame gases, convectional processes will undoubtedly have to be considered as well as diffusional processes.[47] In any event, if a suitable evaporation-rate equation could be derived, it should then be possible to derive an expression for the lifetime of any given particle in the flame. The dimensions of the largest particles are dependent upon the solution concentration and the distribution of droplets produced by the nebulizer,[48,49] and when the lifetime of the largest particle is greater than the time taken for that

particle to reach the height of observation in the flame, the analytical curve will have a smaller slope than the corresponding growth curve.

F. Factors Affecting Aspirator Yield and Solution Transport Rate

Over most analytical concentration ranges the aspirator yield[8 39 50] and the solution transport rate F should be independent of analyte concentration C. At high analyte concentrations, the aspirator yield and solution transport rate will be dependent upon the solution viscosity, surface tension, and solution density.[51] However, for a given aspirator the aspirator yield and solution transport rate are approximately independent of C.

G. Effect of Diffusion on Analyte Concentration

Diffusion of analyte atoms in the flame gases[52 53] should have only a small influence on the curvature of analytical curves.

H. Minimization of Chemical* and Physical* Interferences

It should be stressed that *variations of ϵ, β, F, and e_f will affect the atomic concentration n in exactly the same manner in any flame method.* Because all log B vs. log n curves in flame spectrometry have the same slope (unity) at low concentrations, any change in ϵ, β, F, or e_t in the analytically useful low-concentration region has an identical effect in all flame methods. At high analyte concentrations, the specific log B vs. log n relationship must be used to determine the importance of variations ϵ, β, e_t, or F.

Solute-vaporization interferences (which are often called chemical interferences and which affect ϵ) are generally the most severe ones in flame spectrometry. Such interferences influence the production of atomic vapor and thus the concentration of analyte n. These interferences can often be minimized by using flames that have high temperatures and low rise velocities [long residence times for particles].[54-56]

Ionization interferences (which affect β) are decreased by using low-temperature flames, but such flames increase the importance of solute-vaporization interferences. Because it is often advisable to use high temperature flames to avoid reduction in ϵ, ionization interferences can be minimized by the addition of a high concentration of some ionization suppressor, such as KCl, to all solutions.

If the flame is in local thermodynamic equilibrium, then compound formation does not affect the shapes of the analytical curves of all flame methods. As long as the same flame is used for all measurements and ionization is negligible, the value of β, which reflects the extent of compound formation, will be a *constant for all analyte concentrations.* Of course, by choosing a high temperature flame β can be increased by several orders of magnitude for a given analyte, thereby giving rise to an analytically useful flame spectrometric method. For example, the values of β[39] for many refractory type elements in the C_2H_2/air flame are less than 10^{-5} but approach unity in the C_2H_2/N_2O flame.[57 58]

Finally, interferences affecting F will probably also affect the aspirator yield and can often be minimized in the preparation step: e.g., blood samples may be treated to remove protein or just diluted.[50] Curvature of the analytical curve due to variations in F and aspirator yield with analyte concentration is seldom a problem, because it occurs only at abnormally high concentrations.

V. COMPARISON OF THEORETICAL SIGNAL STRENGTHS

A. Ratios of Radiances in AA or AF and AE

Improvement of detection limits is one of the main goals of all research on flame methods. The actual detection limit depends on factors influencing the signal and the noise and so will strongly vary from element to element and from instrument to instrument. Detailed expressions for estimating limits of detection in AE,[34] AA,[35] and AF[36] [using complex signal-to-noise considerations] are avail-

* Chemical interferences are generally considered to be those influencing ϵ and β; physical interferences are generally considered to be those influencing F and e_t.

able in the literature. These expressions are not only complex but do not clearly indicate the fundamental advantages of each method. Therefore, in this section, the ratios of the radiance (signal) levels in AAL, AAC, AFL, and AFC to those in AE will be given. It is assumed in this section that the noise level in each method is identical, so that the ratio of radiance (signal) levels is the reciprocal of the limits of detection. The ratio is strictly the radiance (signal) gain and is designated G_{SX}, where X is the flame method of analysis which is being compared with AE. This evaluation of G_{SX} can be accomplished by using the low optical density expressions in Table 1. The resulting radiance (signal) gains are

$$G_{SAAC} = \frac{B_{AAC}}{B_{AE}} \simeq \frac{B_{C\lambda_0}}{B_{B\lambda_0}} \tag{39}$$

$$G_{SAAL} = \frac{B_{AAL}}{B_{AE}} = \frac{B_L \delta_0}{c_2 B_{B\lambda_0} \Delta\lambda_D} \tag{40}$$

$$G_{SAFC} = \frac{B_{AFC}}{B_{AE}} \simeq \frac{B_{C\lambda_0} Y \Omega_A}{4\pi B_{B\lambda_0}} \tag{41}$$

$$G_{SAFL} = \frac{B_{AFL}}{B_{AE}} \simeq \frac{B_L \delta_0 Y \Omega_A}{4\pi c_2 B_{B\lambda_0} \Delta\lambda_D} \tag{42}$$

The above equations are valid for signal ratios only if the *same* instrumental system is used for all measurements, if the source is not modulated (if the source is modulated in AA and AF, then the average spectral radiance $B_{C\lambda_0}$ or line radiance B_L must be used), if the same flame is used in all flame methods, if the flame has a constant temperature and concentration of analyte atoms at all points in the measured volume, if the flame area ($L \times l'$) in AA and AF is fully and uniformly illuminated by the source image, if the solid angle $\Omega/4\pi$ subtended by the monochromator in AA is less than or equal to that subtended by the entrance optics, if the same spectrally isolated resonance line is measured in all three methods, and if $L = l$ in AF.

B. Discussion of Radiance- (Signal-) Ratio Expressions

It is interesting to note in Equations 39–42 that the oscillator strength f_{0u} is not explicitly contained in the right-hand expression. Of course, in Equations 40 and 41, f_{0u} is implicitly contained in Y since

$$Y = \frac{A_{u0}}{A_{u0} + \sum_i k_{X_i} n_{X_i}} \tag{43}$$

where A_{u0} is the Einstein coefficient of spontaneous emission in sec^{-1} and is commonly called the transition probability, k_{X_i} is the second-order collisional rate constant in cm^3 sec^{-1}, and n_{X_i} is the concentration of the colliding (quenching) species in cm^{-3}. The summation is over all quenchers. The relationship between A_{u0} and f_{0u}, the absorption oscillator strength, is

$$A_{u0} = \frac{6.62 \times 10^{15} f_{0u} g_0}{\lambda_0^2 g_u} = Z f_{0u} \tag{44}$$

where g_0 and g_u are the statistical weights of the ground and upper states involved in the resonance transition (dimensionless), λ_0 is the peak wavelength) in Å, the number 6 62 x 10^{15} has implied units of $Å^2$ sec^{-1}, and Z is 6.62 $\times$ $10^{15} g_0/\lambda_0^2 g_u$. Combining Equations 44 and 43 gives

$$Y = \frac{f_{0u}}{f_{0u} + \sum_i k_{X_i} n_{X_i} / Z} \tag{45}$$

Thus if Y *is* small compared to unity, it is proportional to f_{0u}, whereas if Y is near unity, it is not a function of f_{0u}. If Y is much less than unity, G_{SAFC} and G_{SFAL} will implicitly depend upon f_{0u}; but if Y is approximately unity, they will be independent of f_{0u}. Therefore the gain factors in Equations 39–42 are only slightly dependent upon the absorption properties of the analyte atoms [Y and δ_0 may be slightly dependent on the absorption properties; $\Delta\lambda_D$ is not critically dependent upon the absorption properties].

The above equations for the G_S factors contain parameters characteristic of the experimental systems alone ($B_{C\lambda_0}$, B_L, Ω, and Ω_A); of the flame alone ($B_{B\lambda_0}$); of the atom and flame ($\Delta\lambda_D$ and Y); and of the atom, flame, and source (δ_0).

C. Evaluation of Parameters in Radiance Ratio-Expressions

Approximate values for all parameters and constants in Equations 39–42 can be given. The constant c_2 is about unity. The term δ_0 is about 0.5[11] for atoms with spectral lines* having a-parameter, of about 0.5 — 2.0 [for $a = 0.5$, $\delta_0 = 0.61$; for $a = 1.0$, $\delta_0 = 0.42$; and for $a = 2\,0$, $\delta_0 = 0.26$]; this should be characteristic of most lines of atoms in flames. The solid angle $\Omega_A/4\pi$ will be about 0.005 at best [this is about one-tenth of the value used by Alkemade[1] in his estimation of gain factors]. Finally, estimates of source spectral radiance for a 450 watt xenon arc continuum (XBO-450) are taken from the paper by Prugger.[59] The xenon lamp values compare well with those of Klein.[60] Estimates of source radiance for high intensity hollow cathode lamps and of high-intensity electrodeless discharge lamps are taken from Prugger[59] and Mansfield et al.,[61] respectively.

The quantum yield Y can be between 0 and 1. For resonance lines in non-hydrocarbon flames diluted with an inert gas, Y will be about 0.5.[18–23] On the other hand, for hydrocarbon flames Y will be of the order of 0.05[18–23] at best. In the comparisons made here Y will be taken as 0.2 as a compromise.

For analytical flames having temperatures of about 2000°K, 2500°K, and 3000°K, the black-body spectral radiance[62] $B_{B\lambda_0}$ (in watts $cm^{-2}ster^{-1}nm^{-1}$) at 2000 Å, 3000 Å, 4000 Å, 5000 Å and 6000 Å are given in Table 2. The values of $B_{C\lambda_0}$ for the 450 watt xenon arc at the same wavelengths[59] are also given in Table 2. The radiances** B_L of high intensity hollow cathode[59] and electrodeless discharge lamps[61] for resonance lines at about 2000 Å (Zn lamp), at about 3000 Å (Mg lamp), at about 4000 Å (Ca or In lamp) and at about 6000 Å (Na lamp) are approximately 10^{-4} to 10^{-5} watt $cm^{-2}ster^{-1}$ for the hollow cathode lamps and about 10^{-2} to 10^{-4} for the electrodeless discharge lamps. For these line sources, average

TABLE 2

Spectral Radiance Values of Black-Body $B_{B\lambda_0}$[62] and 450-W Xenon Arc Source $B_{C\lambda_0}$[59]

Wavelength Å	Spectral Radiance[a,b] $B_{B\lambda_0}$ 2000°K	2500°K	3000°K	$B_{C\lambda_0}$
2000	9E-12	1E-8	1E-6	1E-2
3000	2E-7	2E-5	6E-4	5E-1
4000	2E-5	7E-4	7E-3	1E-0
5000	2E-4	4E-3	3E-2	1E-0
6000	1E-3	1E-2	5E-2	1E-0

a. Units of watt $cm^{-2}ster^{-1}nm^{-1}$
b. E-Notation: 9E-12 means 9×10^{-12}

* It is assumed that the source line width is infinitely narrower than the absorption line width and so δ_0 is evaluated for v = 0 and the a-parameter characteristic of the analyte atoms in the flame gases.

** Note that the units of $B_{C\lambda_0}$, $B_{B\lambda_0}$, and $\Delta\lambda_D$ are still consistent even though they employ a wavelength interval different from that previously given.

values of 5×10^{-5} watt $cm^{-2}ster^{-1}$ for the hollow cathode lamps and 1×10^{-3} watt $cm^{-2}ster^{-1}$ for the electrodeless discharge lamps will be used for calculations. For flames having temperatures between 2000 and 3000°K and for resonance lines between 2000 and 6000 Å, the Doppler half-widths $\Delta\lambda_D$ will be taken as 0.003 nm.[63]

D. Discussion of Calculated Radiance Ratios

Several interesting conclusions can be drawn from the G_S-values estimated in Table 3 using Equations 39–42 and the data listed previously in this section. AF *always must necessarily* result in a smaller signal than AA whether for a line or a continuum source. In fact, for the results given in Table 3, it can be seen that the signal in AAC is 10^3 times as large as in AFC, and that the signal in AAL is 10^3 times as large as in AFL. Because atomic fluorescence results from atomic absorption and because the same instrumental system is assumed, the signal in AA (L or C) is greater than AF (L or C) by the factor $\left(\frac{\Omega_A}{4\pi} Y\right)^{-1}$. *Therefore, if the signals alone are considered, AA (L or C) should be used for the measurement of all analyte atoms having resonance lines shorter than about 6000 Å for essentially all flames* (of course the ratio of signals depends not only on the flame, atom, and line but also on the source type and intensity). Therefore, in terms of signals only, the combination of AA and AE should be used over the analytically useful range of wavelengths.

The data in Table 3 may be somewhat misleading for the case of the 450-watt continuum source. The spectral radiance values used for the XBO-450 lamp are those of Prugger.[59] Our values[33] for a similar lamp are only about one-tenth as large. It is possible that Prugger's values are for an isolated high-intensity region of the arc, whereas our values were averaged over the entire cathode-anode region. If Prugger's values are really for an isolated region, then the G_S-values in Table 3 for AAC/AE and AFC/AE should be divided by a factor of about 10 to be directly comparable.

Although the signals in AF (C or L) are never as great as those in AA (C or L), the values of G_S for AF (C or L) vs. AE can still exceed unity for short wavelength resonance lines. For example, for a 2000°K flame AF results in greater signals than AE for resonance lines shorter than about 6000 Å; the corresponding figures for 2500°K and 3000°K flames are about 4000 Å and 3000 Å, respectively. It is also interesting to note that even if the values for the XBO-450 lamp are ten times as high as they should be (for AFC and AAC), the xenon lamp still should give results comparable with line sources for most resonance lines. Unfortunately, this has not been realized experimentally. The reasons for this are not clear. Finally it should be stressed that the values of G_{SAA} for either continuum or line sources tend to favor AAC and AAL unduly because the solid angle of emission measured in AE is usually much larger than in AAC or AAL; this could mean that the values of G_{SAAC} and G_{SAAL} in Table 3 are about ten times as large as they should be.

VI. COMPARISON OF THEORETICAL LIMITS OF DETECTION IN AE, AA, AND AF

If all noise sources were identical in AE, AA (C or L), and AF (C or L), then the values in Table 3 would be identical with the ratios of the limits of detection in AE vs. AAC, AAL, AFC, or AFL. It is quite reasonable to assume that the noises in AFC, AFL and AE are essentially identical for premixed flames produced using burners with chamber type nebulizers.

A. Total Noise in AE, AFL, and AFC

The total noise N_t, both in AE and in AFL or AFC, is given by

$$N_t = \sqrt{N_{shot}^2 + N_{flame}^2} \quad (46)$$

where N_{shot}, the shot noise at the photodetector output, is a result of the quantum nature of light and the particulate nature of electron emission from the photocathode and depends upon the total light flux reaching the photocathode of the detector, while N_{flame}, the flame flicker noise, is a result of random fluctuations in the background intensity

TABLE 3

Approximate Signal Gain Factors for AAC, AAL, AFC, and AFL Vs. AE for Typical Flame Temperatures and Resonance Line Wavelengths Using Typical Continuum and Line Sources (G_S = Values Calculated Using Equations 39-42 and Using Data Given in Text).

Resonance Line Wavelengths, Å	Flame Temperature											
	2000°K				2500°K				3000°K			
	AAC/AE[a]	AAL/AE[b]	AFC/AE[a]	AFL/AE[b]	AAC/AE[a]	AAL/AE[b]	AFC/AE[a]	AFL/AE[b]	AAC/AE[a]	AAL/AE[b]	AFC/AE[a]	AFL/AE[b]
2000	1E9[c]	2E10(1E8)	1E6	2E7(1E4)	1E6	2E7(1E5)	1E3	2E4(1E1)	1E4	2E5(1E3)	1E1	2E2(1E-1)
3000	2E6	1E6(5E3)	2E3	1E3(5E-1)[c]	2E4	1E4(5E1)	2E1	1E1(5E-3)	1E3	3E2(2E-2)	1E0	3E-1(2E-4)
4000	5E4	1E4(5E1)	5E1	1E1(5E-3)	2E3	3E2(2E0)	2E0	3E-1(2E-4)	2E2	3E1(2E-3)	2E-1	3E-2(2E-5)
5000	5E3	1E2(5E0)	5E0	1E0(5E-4)	2E2	5E1(2E-1)	2E-1	3E-2(2E-5)	3E1	1E1(3E-3)	3E-2	1E-2(3E-5)
6000	1E3	2E2(1E0)	1E0	2E-1(1E-4)	1E2	2E1(1E-1)	1E-1	2E-2(1E-5)	2E1	4E0(2E-4)	2E-2	4E-4(2E-6)

a. Value for XBO-450 xenon arc lamp.
b. First value for electrodeless discharge lamp, second value for high intensity hollow cathode lamp.
c. 1E9 means 1×10^9; 5E-1 means 5×10^{-1}.

emitted by the flame. The latter fluctuations are due to temperature fluctuations in the flame. For the discussion, fluctuations in atomic concentration of analyte due to fluctuations in solution flow rate, aspirator efficiency, and atomization efficiency are assumed to be negligible; in a well-adjusted spectrometric system, they will generally be smaller than the other sources of noise mentioned above and so for simplicity will be omitted from this discussion. In high temperature flames (such as C_2H_2/N_2O, C_2H_2/O_2, and even in H_2/O_2), N_{flame} should be considerably greater than N_{shot} (unless measurements are performed above the luminous portion of the flame, where flame background is minimal). Therefore, the values given in Table 3 for AE, AFC, and AFL should also correspond approximately to the ratios of the detection limit in AE to the detection limits in AFC or AFL (i.e., a value of G_S greater than unity would correspond to detection limit that was larger or, in other words, poorer in AE than in AFC or AFL). It should be stressed that assuming that the same flame is used for AE and AF is not valid experimentally because the most common flame used in AE is now the C_2H_2/N_2O flame, whereas in AF the $H_2/O_2/Ar$ flame appears to be ideal. If different flames with essentially the same temperature and same size are used, then the inverse ratio of limits of detection must also account for the difference in the $\epsilon\beta$ factor in each flame and the increased flame flicker noise in the C_2H_2/N_2O flame.

B. Total Noise in AA

On the other hand, the total noise in AA is given by

$$\underline{N}_t = \sqrt{\underline{N}^2_{shot} + \underline{N}^2_{flame} + \underline{N}^2_{source}} \qquad (47)$$

where N_{source} is the source flicker noise due to fluctuations in the source intensity due to temperature fluctuations, arc wander, wear of electrodes if any are used, fluctuations in vapor concentrations, etc. The source noise has both a white noise component (same noise power per Hz at all frequencies) and a $1/f$ component (increase in noise power per Hz at lower frequencies). In Equation 47, it is also important to note that N_{shot} will be greater for AA than for AE or AF because of the much much greater light flux from the source incident upon the photodetector surface.

C. Evaluation of Total Noise Expressions

The noises in Equations 46 and 47 are assumed to be random (white noise) i.e., the root-mean-square noise voltage is assumed to depend on the square root of the frequency response bandwidth Δf of the measurement system. At frequencies below about 100 Hz, $1/f$ noise (pink noise) is superimposed upon the white noise and so, when using dc or wide-band ac measurement systems, pink noise as well as white noise must be accounted for. Pink noise voltage depends upon $ln\left[\frac{f_1 + \Delta f}{f_1}\right]$, where f_1 is the lower cutoff frequency of the filter system and Δf is the bandwidth.

The shot noise N_{shot}[64] in terms of photodector output is given approximately by

$$\underline{N}_{shot} = \sqrt{2e\underline{Bm}\ \underline{\Delta f}(\underline{i}_d + \underline{i})} \qquad (48)$$

where e is the electron charge, BM is the effective gain of the multiplier photodetector, Δf is the frequency response bandwidth of the measurement device, i_d is the anodic dark current, and i is the total photoanodic signal. For a typical multiplier phototube and measurement system, $2eBM\Delta f$ is about 10^{-13} amperes and i_d is about 10^{-9} amperes.

The photoanodic current due to flame background (assuming an analytically useful spectrometric system) will be of the order of 10^{-9} to 10^{-7} amperes for a low-background flame (H_2/air flame at about 2000°K) and of the order of 10^{-7} to 10^{-5} amperes for a high-background flame (C_2H_2/N_2O flame at about 3000°K). The value of K in the signal expressions was taken to be 1.0 amp watt^{-1}cm^{2}nm ster for a continuum source and 5.0 amp watt^{-1}cm^2 ster for a line source when using a good analytical spectrometric system. Therefore the shot noise current will be of the order of 10^{-11} to 10^{-10} amperes for a low background flame and of the order of 10^{-10} to 10^{-9} amperes for a high background flame.

If, in addition to flame background, an external light source having intensities such as those listed in Table 2 were to be used in AA,

the total photoanodic signal due to both flame and source would be impossibly high, i.e., of the order of 0.01-1 ampere for either low- or high-background flames and for either the continuum xenon source or the high-intensity electrodeless discharge lamps. This is not surprising in view of the direct admittance of the source radiation from such high-intensity lamps into the monochromator. Of course, in such a circumstance one would reduce the slit width, use neutral density filters, utilize a smaller monochromator solid angle Ω, etc., in order to reduce the signal and thus the noise. However, for comparison purposes, it is necessary to compare all of the flame methods under optimal experimental conditions resulting in maximal signal-to-noise ratios. Therefore, for the comparison only, the impossibly high photoanodic current of 0.1 ampere (central value in the range of 0.01–1 ampere) in AAC and AAL will be used. The resulting shot noise for such large photoanodic currents would be of the order of 10^{-7} to 10^{-8} ampere.

Flicker (fluctuation) currents are somewhat difficult to estimate because of the presence of a low-frequency ($1/f$) component as well as the corresponding harmonics and a white noise component.[64] An estimate of flicker noises can be obtained by using $N_{flicker} = \zeta S$, where ζ is the measured ratio of the rms flicker to signal responsible for it and S is the photoanodic signal upon which the flicker is superimposed. For example, for the low (~2000°K)- and high (~3000°K)- temperature analytical flames mentioned above, the flame flicker noise (if $\zeta \sim 0.01$) will be about 10^{-11} to 10^{-9} amperes for the former flames and 10^{-9} to 10^{-7} amperes for the latter flames over most of the wavelength region 2000 to 8000 Å. The source flicker noise ($\zeta \sim 0.001$) or the continuum and line sources discussed above will be about 10^{-5} amperes.

Keeping in mind that the above calculations for noise level are only *approximate* and that only the *relative values* are of much use, we can see that the total noises (see Equation 46 or 47) in AE, AF, and AA are approximately related as follows for low-background flames

$$\underline{N}_{AE} \sim \underline{N}_{AFC} \sim \underline{N}_{AFL} \sim 10^{-5}\ \underline{N}_{AAC} \sim 10^{-5}\ \underline{N}_{AAL} \quad (49)$$

and as follows for high-background flames

$$\underline{N}_{AE} \sim \underline{N}_{AFC} \sim \underline{N}_{AFL} \sim 10^{-3}\ \underline{N}_{AAC} \sim 10^{-3}\ \underline{N}_{AAL} \quad (50)$$

D. Conclusions Concerning Calculated Limits of Detection

Therefore, *if noise as well as signal is accounted for, the limits of detection should be lower for AFL or AFC than for AAL or AAC at all wavelengths when using low-temperature flames. With high-temperature flames, the limits of detection should be comparable for AFL or AFC and for AAL or AAC at all wavelengths.* In any event, if limits of detection are most important, AE should be used for all analyte atoms with resonance lines at wavelengths above *about* 3000 Å, but AF or AA should be used for all analyte atoms with resonance lines at wavelengths below about 3000 Å, with high-temperature, high-background flames. High-temperature flames are the ones of greatest analytical utility because they minimize solute-vaporization interferences. Therefore, on purely theoretical grounds, it would seem to be immaterial whether AFL (or AFC) or AAL (or AAC) were used with high-temperature flames. However, because essentially the same spectrometric measurement system can be used for both AF and AE, it would seem that the combination of AF and AE would be ideal for experimental work. With low-temperature flames, the choice is more obviously AF and AE.

L'vov[65] has also compared the relative limits of detection of AA and AF, and Alkemade has also compared those of AE and AA[12] and of AF and AE.[1]

VII. COMPARISON OF EXPERIMENTAL SENSITIVITIES OF AE, AA AND AF

In Table 4, a tabulation of the best (lowest) currently available experimental limits of detection by AFL, AAL, and AE is presented. In Table 5, a similar listing is given for AFC, AAC, and AE. It is evident from these tables that at the present time the *limits of detection*

TABLE 4

Comparison of Experimental Limits of Detection in AAL, AFL, and AE

Part I. Elements Determined by AAL, AFL, and AE

Element	Wavelength (Flame)[a]			Limits of Detection (μg/ml)		
	AAL(A)	AFL(A)	AE(A)	AAL [66]	AFL	AE
Ag	3281 (A/A)	3281 (H/A)	3281 (A/N)	5E − 4[b]	1E − 4 [67]	2E − 2 [68]
Al	3962 (A/N)	3962 (H/N)	3962 (A/N)	1E − 1	5E + 1 [69]	5E − 3 [70]
As	1937 (H/A)	1937 (H/A)	2350 (A/O)	1E − 1	1E − 1 [71]	5E + 1 [72]
Au	2428 (A/A)	2676 (H/A)	2676 (A/N)	2E − 2	5E − 2 [73]	4E − 0 [72]
Be	2349 (A/N)	2349 (A/N)	2349 (A/N)	2E − 3	1E − 2 [74, 75]	1E − 1 [74]
Bi	2231 (A/A)	2231 (H/A)	2231 (A/O)	5E − 2	5E − 2 [76]	2E − 0 [77]
Ca	4227 (A/A)	4227 (H/A)	4227 (A/N)	2E − 3	2E − 2 [67]	1E − 4 [68]
Cd	2288 (H/A)	2288 (H/O)	3261 (A/N)	1E − 2	1E − 6 [67]	2E − 0 [68]
Co	2407 (A/A)	2407 (H/A)	3274 (A/N)	5E − 3	1E − 2 [78]	5E − 2 [68]
Cr	3579 (A/A)	3579 (H/A)	3454 (A/N)	5E − 3	5E − 2 [71]	5E − 3 [68]
Cu	3247 (A/A)	3247 (H/A)	4254 (A/N)	5E − 3	1E − 3 [79]	1E − 2 [68]
Fe	2483 (A/A)	2483 (H/A)	3720 (A/N)	5E − 3	8E − 3 [71]	5E − 2 [68]
Ga	2874 (A/A)	4172 (H/A)	4172 (A/N)	7E − 2	3E − 1 [71]	1E − 2 [68]
Ge	2652 (A/N)	2652 (H/A)	2652 (A/N)	1E − 0	2E + 1 [73]	5E − 1 [68]
Hg	2537 (A/A)	2537 (H/A)	2537 (A/O)	5E − 1	2E − 2 [80]	4E + 1 [72]
In	3039 (A/A)	4511 (H/A)	4511 (A/N)	5E − 2	1E − 1 [67]	2E − 1 [70]
Mg	2852 (A/A)	2852 (A/A)	2852 (A/N)	3E − 4	1E − 3 [81]	5E − 3 [68]
Mn	2795 (A/N)	2795 (H/A)	4031 (A/N)	2E − 3	6E − 3 [67]	5E − 3 [68]
Ni	2320 (A/A)	2320 (H/A)	3415 (A/N)	5E − 3	3E − 3 [78]	6E − 1 [72]
Pb	2833 (A/A)	4058 (H/A)	4058 (A/N)	1E − 2	1E − 2 [73]	2E − 1 [68]
Rh	3435 (A/A)	3692 (H/A)	3692 (H/A)	3E − 2	3E − 0 [73]	3E − 1 [72]
Sb	2175 (A/A)	2311 (P/A)	2598 (A/O)	1E − 1	5E − 2 [82]	2E + 1 [72]
Se	1960 (H/A)	1960 (A/A)	—	1E − 1	1E − 0 [83]	—
Sn	2246 (H/A)	3034 (H/A)	2840 (A/N)	3E − 2	5E − 2 [84]	3E − 1 [68]
Sr	4607 (A/A)	4607 (H/A)	4607 (A/N)	1E − 2	3E − 2 [67]	2E − 4 [68]
Te	2143 (A/A)	2143 (A/A)	2383 (A/O)	1E − 1	5E − 2 [85]	2E + 2 [72]
Tl	2768 (A/A)	3776 (H/A)	3776 (A/N)	3E − 2	8E − 3 [67]	2E − 2 [68]
Zn	2138 (A/A)	2138 (H/A)	2138 (A/O)	2E − 3	4E − 5 [67]	5E + 1 [72]

Part II. Elements Determined by AAL and AE

Element	Wavelength (Flame)[a]			Limits of Detection (μg/ml)		
	AAL(A)	AFL(A)	AE(A)	AAL [66]	AFL	AE
B	2498 (A/N)	—	2498 (A/N)	6E − 0	—	3E + 1 [72]
Ba	5536 (A/N)	—	5536 (A/O)	5E − 2	—	2E − 3 [72]
Ce	—	—	5697 (A/O)	—	—	1E + 1 [72]
Cs	8521 (A/A)	—	8521 (A/O)	5E − 2	—	8E − 3 [72]
Dy	4212 (A/N)	—	4046 (A/N)	2E − 1	—	7E − 2 [86]
Er	4008 (A/N)	—	4008 (A/N)	1E − 1	—	4E − 2 [86]
Eu	4594 (A/N)	—	4594 (A/N)	4E − 2	—	6E − 4 [86]
Gd	3684 (A/N)	—	4402 (A/N)	4E − 0	—	2E − 0 [86]
Hf	3073 (A/N)	—	3682 (A/O)	8E − 0	—	8E + 1 [72]
Ho	4104 (A/N)	—	4054 (A/N)	1E − 1	—	2E − 2 [86]
Ir	2640 (A/A)	—	3800 (A/O)	2E − 0	—	1E + 2 [72]
K	7665 (A/A)	—	7665 (A/O)	5E − 3	—	3E − 3 [72]
La	5501 (A/N)	—	5791 (A/N)	2E − 0	—	2E − 0 [68]
Li	6708 (A/A)	—	6708 (A/N)	5E − 3	—	3E − 5 [68]
Lu	3312 (A/N)	—	3312 (A/O)	3E − 0	—	2E − 1 [72]
Mo	3133 (A/A)	—	3903 (A/N)	3E − 2	—	1E − 1 [68]
Na	5890 (A/A)	—	5890 (A/O)	2E − 3	—	1E − 4 [72]
Nb	3344 (A/N)	—	4059 (A/N)	3E − 0	—	6E − 2 [87]
Nd	4634 (A/N)	—	4925 (A/N)	2E − 0	—	2E − 1 [86]
Os	2909 (A/N)	—	4420 (A/O)	1E − 0	—	1E + 1 [72]
Pd	2476 (A/A)	—	3635 (A/N)	3E − 2	—	5E − 2 [68]

Part II. Elements Determined by AAL and AE

Element	Wavelength (Flame)[a]			Limits of Detection (μg/ml)		
	AAL(A)	AFL(A)	AE(A)	AAL[66]	AFL	AE
Pr	4951 (A/N)	—	4951 (A/N)	1E + 1	—	1E − 0 [86]
Pt	2660 (A/A)	—	2660 (A/N)	1E − 1	—	2E − 0 [68]
Rb	7800 (A/A)	—	7800 (A/O)	5E − 3	—	2E − 3 [72]
Re	3460 (A/N)	—	3460 (A/N)	1E − 0	—	1E − 0 [72]
Ru	3499 (A/A)	—	3728 (A/O)	3E − 1	—	3E − 1 [72]
Sc	3912 (A/N)	—	3912 (A/N)	1E − 1	—	3E − 2 [68]
Si	2516 (A/N)	—	2516 (A/O)	1E − 1	—	5E − 0 [72]
Sm	4297 (A/N)	—	4760 (A/N)	2E − 0	—	2E − 1 [86]
Ta	2715 (A/N)	—	4813 (A/O)	5E − 0	—	2E + 1 [72]
Tb	4327 (A/N)	—	4319 (A/N)	2E − 0	—	4E − 1 [86]
Th	—	—	5761 (A/O)	—	—	2E + 2 [72]
Ti	3643 (A/N)	—	3999 (A/N)	1E − 1	—	2E − 1 [68]
Tm	3718 (A/N)	—	3718 (A/N)	2E − 1	—	2E − 2 [86]
U	3515 (A/N)	—	5915 (A/O)	3E + 1	—	1E + 1 [72]
V	3184 (A/N)	—	4379 (A/N)	2E − 2	—	1E − 2 [68]
W	4009 (A/N)	—	4009 (A/N)	3E − 0	—	5E − 1 [68]
Y	4077 (A/N)	—	3621 (A/N)	3E − 1	—	4E − 2 [86]
Yb	3988 (A/N)	—	3988 (A/N)	4E − 2	—	2E − 3 [86]
Zr	3601 (A/N)	—	3601 (A/N)	5E − 0	—	5E + 1 [72]

a. Flame types: A/A = acetylene/air; A/N = acetylene/nitrous oxide; A/O = acetylene/oxygen; H/A = hydrogen/air; H/O = hydrogen/oxygen; P/A = propane/air. The ratio of fuel oxidant is not specified; also in several flames the oxidant is entrained air).

b. 5E − 4 means 5×10^{-4}.

are much lower with line sources than with continuum sources in AA and AF. This is somewhat surprising when one calculates signal ratios and signal-to-noise ratios such as those discussed in the previous two sections. The authors have *no* explanation for the relatively poor experimental detection limits with continuum sources (especially in AA). Even if the xenon XBO-450 intensity estimate is ten times too high and the geometry is only one tenth as favorable as was assumed, it would seem that the continuum sources in AA and AF should give better limits of detection when using sources with radiances listed in Table 2.

From the results in Table 4, it is apparent that the useful combinations are those of AE with AFL or AAL, i.e., AE is complementary with AFL or AAL if *high temperature* flames[68 70 74 93-95] are employed. Once again, because AE and AFL can utilize the same instrumental system and also result in lower detection limits if *low-temperature* flames are used, the combination of AE with AFL seems to be most ideal at the present time. However, if experimental limits of detection in AFC ever approach the theoretical values, then the *ideal combination* would be AE and AFC where a *single scanning spectrometric system with dc readout* could possibly be used for all elements with resonance lines between 2000 and 8000 Å.

From a comparison of the data in Table 4 for all elements which have been reliably studied by AE, AAL, and AFL (including the alkali metals, which should give poorer detection limits by AFL than AE, although no data are available), it can be seen that AFL is superior* to AAL and AE for Ag, Cd, Cu, Hg, and Zn; AAL is superior to AFL and AE for Be, Mg, and Rh; AE is superior to AAL and AFL for Cs, Ga, In, K, Li, Na, Rb, and Sr; AAL and AFL are superior to AE for As, Au, Bi, Co, Fe, Ni, Pb, Sb, Se, Sn, and Te; AAL and AE are superior to AFL for Ca and Cr; and AAL, AFL, and AE are comparable to each other for Ge, Mn, and Tl. In all cases, when comparable data are available, AFC and AAC resulted in substantially poorer limits of detection.

* Superior means that the detection limit is less than one-third of the lowest value listed for the other flame spectrometric methods.

TABLE 5

Comparison of Limits of Detection in AAC, AFC, and AE.

Element	Wavelength (Flame)[a]			Limits of Detection (μg/ml)[b]		
	AAC(A)	AFC(A)	AE	AAC	AFC	AE
Ag	3281(A/O)	3281(H/A)	3281(A/N)	2E − 1[b] [88]	1E − 3 [89]	2E − 2 [68]
Al	3944(A/O)	—	3962(A/N)	2E − 0 [88]	—	1E − 2 [69]
Au	—	2676(H/O)	2676(A/N)	—	4E − 0 [90]	5E − 1 [68]
Ba	5536(A/O)	—	5536(A/O)	9E − 1 [88]	—	3E − 2 [72]
Bi	3068(A/O)	3068(H/O)	2231(A/O)	4E − 0 [88]	2E − 0 [90]	4E + 1 [68]
Ca	4227(A/O)	4227(H/A)	4227(A/N)	3E − 2 [88]	1E − 1 [91]	1E − 4 [68]
Cd	2288(A/O)	2288(H/O)	3261(A/N)	1E − 2 [92]	8E − 2 [90]	2E − 0 [68]
Co	3527(A/O)	2407(H/A)	3454(A/N)	3E − 0 [88]	5E − 1 [91]	5E − 2 [68]
Cr	3579(A/O)	3579(H/A)	4254(A/N)	2E − 1 [88]	1E + 1 [73]	5E − 3 [68]
Cs	8521(A/O)	—	8521(A/O)	2E − 1 [88]	—	8E − 3 [72]
Cu	3247(A/O)	3247(H/A)	3274(A/N)	5E − 2 [88]	2E − 2 [89]	1E − 2 [68]
Dy	4212(A/O)	—	4212(A/O)	5E − 1 [88]	—	1E − 1 [72]
Er	4008(A/O)	—	4008(A/O)	1E − 0 [88]	—	3E − 1 [72]
Eu	4627(A/O)	—	4594(A/O)	4E − 1 [88]	—	3E − 3 [72]
Fe	3720(A/O)	2483(H/A)	3720(H/A)	1E − 0 [88]	1E − 0 [73]	5E − 2 [68]
Ga	2814(A/O)	4172(H/A)	4172(A/N)	2E − 0 [88]	5E − 0 [73]	1E − 2 [68]
Gd	4079(A/O)	—	4520(A/O)	6E − 1 [88]	—	2E − 0 [72]
Ho	4163(A/O)	—	4104(A/O)	2E− 0 [88]	—	1E − 1 [72]
In	3039(A/O)	4105(H/A)	4511(A/N)	2E − 1 [88]	2E − 0 [73]	5E − 3 [68]
Ir	—	2544(H/A)	3800(A/O)	—	1E + 2 [73]	1E + 2 [72]
K	7665(A/O)	—	7665(A/O)	3E − 2 [88]	—	3E − 3 [72]
Li	6708(A/O)	—	6708(A/N)	4E − 3 [88]	—	3E − 6 [72]
Lu	3312(A/O)	—	3312(A/O)	5E + 1 [88]	—	2E − 1 [72]
Mg	2852(A/O)	2852(H/A)	2852(A/N)	1E − 2 [88]	1E − 2 [91]	5E − 3 [68]
Mo	3133(A/O)	—	3903(A/N)	8E − 1 [88]	—	1E − 1 [68]
Na	5890(A/O)	—	5890(A/N)	3E − 2 [88]	—	1E − 4 [72]
Nb	4059(A/O)	—	4059(A/N)	3E + 1 [88]	—	1E − 0 [68]
Nd	4925(A/O)	—	4925(A/O)	4E + 1 [88]	—	1E − 0 [72]
Ni	3415(A/O)	2320(H/A)	3415(A/N)	7E − 1 [88]	1E − 0 [89]	6E − 1 [72]
Pb	2833(A/O)	4058(H/A)	4058(A/N)	2E − 0 [88]	3E − 0 [73]	2E − 1 [68]
Pd	—	3405(H/A)	3635(A/N)	—	5E + 1 [73]	5E − 2 [68]
Pr	4951(A/O)	—	4940(A/O)	6E + 1 [88]	—	2E − 0 [72]
Pt	—	2660(H/A)	2660(A/N)	—	5E + 2 [73]	4E + 1 [72]
Rb	7800(A/O)	—	7800(A/O)	4E − 2 [88]	—	2E − 3 [72]
Re	3460(A/O)	—	3460(A/N)	5E − 0 [88]	—	2E − 1 [68]
Rh	—	3692(H/A)	3692(A/O)	—	1E + 1 [73]	3E − 1 [72]
Ru	—	3728(H/A)	3728(A/O)	—	1E + 2 [73]	3E − 1 [72]
Sb	—	2311(H/A)	2598(A/O)	—	3E + 2 [73]	2E + 1 [72]
Sc	3912(A/O)	—	3912(A/N)	1E − 0 [88]	—	3E − 2 [68]
Sn	2863(A/O)	—	2840(A/N)	6E − 0 [88]	—	3E − 1 [68]
Sr	4607(A/O)	—	4607(A/N)	6E − 2 [88]	—	2E − 4 [68]
Tb	4327(A/O)	—	4327(A/O)	3E + 1 [88]	—	1E − 0 [72]
Ti	3653(A/O)	—	3999(A/N)	5E − 0 [88]	—	2E − 1 [68]
Tl	2768(A/O)	3776(H/A)	3776(A/N)	6E − 1 [88]	7E − 2 [89]	2E − 2 [68]
Tm	4094(A/O)	—	4106(A/O)	1E − 1 [88]	—	2E − 1 [72]
V	3184(A/O)	—	4379(A/N)	6E −1 [88]	—	1E − 2 [68]
Y	4077(A/O)	—	4077(A/N)	1E + 1 [88]	—	1E − 0 [68]
Yb	3988(A/O)	—	3988(A/O)	2E − 1 [88]	—	5E − 2 [72]
Zn	2138(A/O)	2138(H/A)	2138(A/O)	2E − 2 [92]	3E − 2 [91]	5E + 1 [72]

a. See footnote a in Table 4.
b. 2E − 1 means 2×10^{-1}.

VIII. COMPARISON OF EXPERIMENTAL SELECTIVITIES OF AE, AA, AND AF

A. Spectral Interferences

The spectral interferences in AAL and AFL should be less than in any other of the five flame methods (AE, AAL, AAC, AFL, and AFC) because interference can occur only when there is overlap between the analyte resonance line and the interferent. Although this type of interference is possible[96] in AAL and AFL, it is not too important because the absorption lines are narrow (approximately 0.1 Å with wings extending out several Å) and because the absorption is relatively small unless the lines overlap significantly or unless the interferent has a very large absorption coefficient even in the line wings where small overlap may occur.[58 96-98]

The spectral interferences in AE, AAC, and AFC should be approximately identical because any substance will interfere in these techniques if it has spectral lines or bands within the spectral bandwidth of the monochromator. In AFC direct line or stepwise line[6 99] fluorescence can also cause interference, but this should be relatively unimportant compared to the direct interference of an element with a resonance line within the spectral bandwidth of the monochromator which includes the resonance line of the analyte. It should be stressed that spectral interferences in AE, AAC, and AFC become less significant as the spectral bandwidth s of the monochromator is reduced. Assuming that a good medium-resolution monochromator is used ($s \sim 0.2$ Å), *spectral interferences should be only slightly greater in AE, AAC, AFC than in AAL and AFL.*

B. Chemical Interferences

These are interferences which affect β and ϵ (solute vaporization) and therefore have exactly the same effect on all flame methods. They are generally the most severe interferences in flame spectrometric methods.

C. Flame-Temperature-Variation Interferences

The variation of flame temperature has little effect on any of the important parameters except for the Boltzmann factor $\exp(-hc/\lambda_0 kT_F)$ and the β factor. Assuming that the analysis deals with analyte concentrations in the middle linear part of the analytical curve, ionization is negligible and only compound formation needs to be considered. The β factor is much more sensitive to flame temperature variation than other factors such as Y, $\Delta\lambda_0$, δ_0, ϵ, e_f, etc., because the β-factor also depends upon an exponential term similar to the Boltzmann factor except the hc/λ_0 is replaced by V_d, the dissociation energy of the stable molecule formed between the analyte atoms and the flame gas products X. As a first approximation, the most stable molecular entity for most analytes in most analytical flames is the monoxide (in some cases the monohydroxide may be stable, but this does not affect the present discussion).

In AE the relative change in signal, dS_{AE}, with change in flame temperature, dT_F, is found [100] to be

$$\frac{dS_{AE}}{S_{AE}} \simeq \left(\frac{E_u + V_d}{kT_F}\right)\frac{dT_F}{T_F} \qquad (51)$$

where S_{AE} is the signal itself, and E_u is the excitation energy of the resonance transition ($E_u = hc/\lambda_0$). For AAL, AAC, AFL, and AFC, it can be shown[100] that

$$\frac{dS_{AA}}{S_{AA}} = \frac{dS_{AF}}{S_{AF}} = \left(\frac{V_d}{kT_F}\right)\frac{dT_F}{T_F} \qquad (52)$$

The above equations are valid only if V_d is at least about 2.5 eV and for analytical flames (temperature between 2000 and 3500°K). Because nearly all elements form monoxides with dissociation energies greater than about 2.5 eV, the above equations can be used to give gross estimates of temperature sensitivity. The ratio of the sensitivities of AE and AA or AF to flame-temperature change (assuming the same flame is being used for a given analyte) is given by

$$\gamma = \frac{dS_{AE}/S_{AE}}{dS_{AA}/S_{AA}} = \frac{dS_{AE}/S_{AE}}{dS_{AF}/S_{AF}} = \frac{E_u + V_d}{V_d} \qquad (53)$$

As long as the value of V_d is at least about 6 eV (monoxides of Al, B, Ce, Dy, Er, Gd,

Ge, Hf, Ho, La, Lu, Nb, Pr, Sc, Si, Sm, Sn, Ta, Tb, Th, Ti, Tm, U, V, Y and Zr), the relative sensitivity factor γ will vary from less than 10/6 for a line at 4000 Å to less than 7.5/6 at 8000 Å. For such elements, *AE is really not much more sensitive to flame temperature variation than either AA or AF methods.* If ionization is also a problem, the temperature dependences of ionization and compound formation must be considered. If both ionization and compound formation are important, β may be approximately constant with temperature change. Under such unusual circumstances, AE is much more temperature sensitive than AA or AF, but because ionization can be minimized by use of an ionization buffer such as KCl, this situation is seldom important. Therefore the problem of flame-temperature variation in AE (sometimes called excitation interference) *has been grossly overstated in books and articles stressing the advantages of AA and the limitations of AE.*

It should be further stressed that there is *no such thing as energy-transfer interference in AE if the flame is, indeed, in thermal equilibrium.* This is necessitated by the law of detailed balance. Energy-transfer interferences have again been stressed as limitations in AE when authors are comparing AA with AE. Alkemade[12] has shown that this type of interference is indeed just a fantasy.

D. Physical Interferences

These are interferences that affect ϵ (aspirator yield) and F and therefore, again, have exactly the same effect on all flame methods. These interferences are generally not as disastrous as chemical interferences but, nevertheless, are extremely important. A reduction of both chemical and physical interferences results in more reliable analyses by all flame methods.

E. Scattering and Band Absorption of Exciting Radiation in AA and AF

These interferences are *not* present in AE. Such interferences result in an increased absorption and fluorescence signal and a slight increase in total noise in the instrumental system. Because these interferences are spectrally continuous, the increased signals can be compensated for in AAC and AFC by simply scanning the wavelength region containing the spectral line. The signal increase in AA is primarily a result of molecular absorption.[101-105] Scattering results in little effective absorption because of the use of premixed flames and efficient nebulizers in AA. The signal increase in AF is a result of scattering of exciting radiation from incompletely vaporized particles within the excitation region of the flame gases: these are especially likely to appear when total-consumption nebulizer burners and turbulent flames are used, but are generally present to some extent even in premixed flames with chamber-type nebulizers.[106]

In AAL, molecular absorption[101-105] can be compensated for by measuring the absorbance at a line whose wavelength is near that of the resonance line. One may instead use a continuum light source set at the resonance line to determine the effective absorbance due to molecular absorption (if the spectral bandwidth is much greater than the absorption line width, atomic absorption at the resonance line is small compared to molecular absorption). Some commercial instruments allow this correction to be made automatically.

In AFL, the scattering signal can be measured using a nearby nonfluorescence line of similar intensity to the resonance line or by using a control sample. The control sample must be similar in matrix concentration and composition to the unknown to achieve a good correction. Of course, if a high-temperature low-rise-velocity flame with an efficient nebulizer were used, scattering due to particles should be negligible. It is always best to go to the source of the problem if possible.

F. Quenching Interferences in AF

Quenching of excited atoms due to change in flame gas composition caused by introducing the nebulized sample solution into the flame can only produce an interference in AF. In AE, there are as many exciting collisions as quenching collisions as long as thermal equilibrium approximately prevails. In AA, the mechanism of deactivation is irrelevant (see discussion under burner types). However, it is well known that substitution of argon for nitrogen as a diluent in a premixed air/H_2

flame gives rise to enhanced fluorescence signals as a result of the lower quenching cross section of argon. It might, therefore, be assumed that quenching could result in a specific interference in AF. Smith[108] has discussed this problem, and the discussion given here is taken from his chapter. The total pseudo-first-order quenching rate $\left(\sum_i k_{X_i} n_{X_i}\right)$ for typical flame-gas species with the Na-D lines and for a dry air-propane flame (1800°K) is 15.5×10^8 sec^{-1}. For Na, A_{u0} is 0.63×10^8 sec^{-1} and so Y [see Equation 43] is 0.039. Now to change Y by ± 0.001, the total quenching rate would have to be changed by $\pm 0.4 \times 10^8$ sec^{-1}. If the species introduced with the sample has the same second-order collisional rate constant as N_2 ($k_{N_2} n_{N_2} = 11.1 \times 10^8$ sec^{-1}), this change would correspond to a proportion of the interferent which is about 3.6% of the nitrogen concentration in the flame gases or about 2.8% of the total flame gas composition. In this calculation, the introduction of solvent water is neglected, and it is assumed that the interferent is no more efficient as a quencher than N_2. Certainly it is unlikely that any component at concentrations less than about 10^4 ppm introduced into the flame can result in any reasonably measurable quenching interference.

IX. COMPARISON OF INSTRUMENTATION IN AE, AA, AND AF

A. Basic Instrumental Systems in AE, AA, and AF

Very similar instrumentation is used in AE, AA, and AF (see Figure 1). All flame spectrometers utilize a flame, a monochromator, a photodetector, and a current-measurement device and readout. Unfortunately, many comparisons of AA and AE have been made on the basis of the most modern equipment and flames available for AA and the antiquated equipment and flames used 20 years ago in AE. Of course, in AA and AF, an external light source is needed to excite the atomic vapor in the flame, and this necessarily adds complexity to the equipment. In the case of AA, entrance optics are needed to focus an image of the source upon the flame (see Figure 1). In AF, additional entrance optics are required to form an image of the source upon the flame cell (right angle arrangement, see Figure 1). More elaborate electronic systems and modulated light sources have been used in AA and AF in order to minimize the response to thermal emission in the flame. Actually, this is only necessary above about 3000 Å because thermal emission is generally small below this wavelength. Dc electronic systems have been used with good success for AFL[75 79 80 90 95] and were used in the early stages of development of AAL.[106 109-111] With a dc electronic system and unmodulated source, a greater signal is obtained. Of course, with a dc system electronic drift and measured noise can be more severe. Noise is more severe because of the presence of both white noise and $1/f$ noise. By modulating the light source (mechanically or electronically) and using an ac amplifier or, better yet, a phase-sensitive amplifier locked in to a modulating frequency greater than about 100 Hz, drift and $1/f$ noise are minimized; of course, the signal is generally reduced at least 50%. In both dc and ac systems, damping (RC) circuits can be utilized to narrow the instrument bandwidth Δf. In addition, in a dc system the signals of interest are measured on top of the flame background. The above differences in the instrumentation previously used in AE, AA, and AF are rather minor compared to the more basic differences in terms of burner types and geometry of entrance optics, flame type, and sources of excitation used in AA and AF. The possible use of the three methods in multielement analysis will also be discussed in this section.

B. Flame Type, Flame Shape, and Geometry of Entrance Optics

The *optimum flame in AE* should be that which results in the largest value of $nle^{-Eu/kT}/N_t$. The optimum flame type and burner are most likely a premixed laminar flame of C_2H_2/N_2O produced using a long-path-length burner. The C_2H_2/N_2O flame appears to be optimal because of its high temperature and low burning velocity, which result in maximum excitation and minimum solute-vaporization interferences. By means of effi-

cient nebulizers, it should be possible to obtain a value of ϵ that is larger than it was for the turbulent flames produced by the total consumption nebulizer burners used almost exclusively in the past for AE studies.[50 112 113] Because a premixed flame with an efficient nebulizer suffers little change in temperature[114] upon nebulization of solvent, such flames, especially those obtained with an outer flame sheath,[111] have higher and more uniform temperatures than the inherently hotter flames of C_2H_2/O_2 or H_2/O_2 produced using total-consumption nebulizer burners and aspirating water solutions. Therefore the average β-values of most atoms should be greater in premixed than in turbulent flames. It should be mentioned that β-values of easily ionized atoms can be considerably reduced in such hot flames, and so it may be necessary in those cases to add an ionization suppressor. Of course, ionization interferences can be reduced by going to low-temperature flames (such as H_2/air or C_2H_2/air), but this often results in great losses in sensitivity and selectivity.

The rates of flow of sample solution into the chamber in premixed flames or directly into the flame in turbulent flames should be similar (actually F is usually greater for premixed flames). Finally, the l- factor for a long path length flame can be of the order of ten times that for a turbulent flame produced using a total-consumption nebulizer burner. It should be stressed, however, that the produce ϵl is limited for any premixed burner system. If l is increased beyond a certain value, the efficiency of aspiration will decrease, there will be little change in ϵl, and the flame stability will be poorer.

The premixed-type flame produced using the total-consumption nebulizer burner[95] is a compromise between the optimum flame-burner system discussed above and the turbulent flame with the total-consumption nebulizer burner. Such a premixed flame most likely results in greater ϵ values and has a lower flame background than the corresponding turbulent flames. In addition, such a flame-burner system is certainly simpler, safer, and more versatile than the optimal flame discussed above and should not be dismissed lightly.

The best *entrance optics design for AE* is that which just fills the monochromator optics with a solid angle of radiation.[115] If dark current shot noise is the limiting noise, then the signal-to-noise ratio can be increased by collecting more than one solid angle of radiation (at least up until the point where flame-flicker noise is limiting[34]). Another advantage of a homogeneous flame (the optimal flame with sheath) and an efficient nebulizer is that there is no limitation on the size of the solid angle collected [with inhomogeneous flames, one must be cautious in the size of the image and the solid angle of radiation collected because of the variation in ϵ and β as well as flame background and flicker].

In AA, the *optimal flame-burner system* should be one maximizing nl/N_t. The optimum flame type and shape are therefore most likely the C_2H_2/N_2O flame produced with a long path length burner and an efficient nebulizer (also with a flame sheath). In such a homogeneous flame, the size of the image of the source upon the flame is not critical as long as the source image is within the confines of the flame cell. If the flame has a large temperature gradient (no flame sheath) and if nebulization is inefficient, then the source image size is limited to the flame area giving the maximum value of nl/N_t.

The *best entrance optics* are generally those that collect the smallest solid angle of radiation from the flame and yet provide sufficient radiant flux at the photodetector. Such a system minimizes thermal emission pickup. However, such a system could possibly result in interference from the atomic fluorescence resulting from atomic absorption. Most workers in AA do not know of this potential interference or do not worry about it. It is therefore interesting to make a calculation for an actual system to determine the extent of such an interference. According to Pearce, de Galan, and Winefordner,[20] the fraction of radiation absorbed is decreased by the following factor due to atomic fluorescence

$$\alpha = \alpha_A \left[1 - \frac{Y\ \Omega\ \Theta_s}{4\pi\ \Theta_f}\right] \qquad (54)$$

where Y is the quantum yield of the fluorescence, Ω is the solid angle of radiance incident

upon the monochromator, θ_s is the area of the image of the source of excitation upon the entrance slit of the monochromator, θ_f is the area of fluorescence emission in the direction of the monochromator, and α_Λ is the fraction of radiation absorbed in the absence of atomic fluorescence. For a typical AA system, $\Omega \sim 0.04$ sterad, $\theta_s \sim 0.5$ cm² and $\theta_f \sim 0.5$ cm². Even if $Y \approx 1$, the correction factor $Y\Omega\theta_s/4\pi\theta_f$ is only 0.003, so that the fraction of radiation absorbed is 0.997 α_Λ; the error would not be detectable by most instrumental systems.

In AF, the best flame-burner system is most likely a combination of C_2H_2/N_2O and $H_2/O_2/Ar$ using a rectangular flame with a premix burner, an efficient nebulizer (a flame sheath around each flame is also desirable) and complete illumination of the flame and measurement of the fluorescence as in Figure 2-(3). In AF, the factor nLY/N_t must be maximized. For the same burner configuration and nebulizer, only $\epsilon\beta Y/N_t$ will depend upon the flame type used. The factor $\epsilon\beta$ will most likely be larger for refractory type elements in the C_2H_2/N_2O flame than in the $H_2/O_2/Ar$ flame. However, Y/N_t will be considerably greater in a flame of the latter type than in hydrocarbon flames (see Table 6 for several Y-values taken from the measurements of Hooymayers and Alkemade[16 18 19] and Jenkins.[21 22])

C. Sources of Excitation in AA and AF

The most used line sources in AAL are the high-brightness shielded hollow cathode and high-intensity hollow cathode lamps; in AFL they are microwave-excited electrodeless discharge lamps and high intensity hollow cathode lamps.

Hollow cathode lamps of the shielded variety have been made for about 70 elements. These devices are simpler in construction, less expensive, and simpler to operate than, and are nearly as intense as, the high-intensity lamps which require several power supplies. Difficulties arise in some shielded hollow cathode lamps for metals with low melting points. Multielement cathodes generally are considerably less intense than single-element cathodes and also yield analytical results more prone to interference effects. Multicathode and demountable hollow cathode lamps have found little use in routine AA studies.

High-intensity lamps have been used with good results in both AA[106 109-111 116 117] and AF.[78 118-120] Such lamps produce reasonably intense and stable radiation for limited numbers of elements. The lamps and associated power supplies are expensive and so have not found much use in AA or AF as compared to shielded hollow cathode lamps in AA and electrodeless discharge lamps in AF.

Electrodeless discharge lamps[61 67 121-123] with

TABLE 6

Fluorescence Quantum Yields, Y, for Na and K in C_2H_2/Air and $H_2/O_2/Ar$ Flames.

	Y	
	C_2H_2/Air	$H_2/O_2/Ar$
Na (23)	0.040 (2200°K)[a]	0.74 (2:1:9.7–1800°K)[b]
Na (23)	0.044 (2400°K)[a]	0.60 (1:1:9.7–1800°K)[b]
Na (20)	0.030 (2600°K)[a]	0.32 (2:1:3.45–2070°K)[b]
K (20)	0.023 (1700°K)[c]	0.64 (2:1:3.45–2070°K)[b]

a. Flame temperature in parenthesis.
b. Volume ratio and temperature in parenthesis.
c. Flame is $CO:O_2:Ar$ in volume ratio 3:0.5:4.

intensities much greater than that of even the high-intensity hollow cathode lamp have been prepared for a limited number of elements. The technology of preparing and operating such lamps is currently limited. Electrodeless discharge lamps have the advantages of high spectral radiance and low cost of preparation. Unfortunately, much time and difficulty in tuning such lamps are necessary to achieve a high, relatively constant intensity. In addition, these lamps are sometimes considerably less stable than hollow cathode lamps and have much shorter lifetimes. Much development research needs to be performed in the area of preparation and operation of electrodeless discharge lamps in order to obtain intense, stable, long-lived lamps.*

Although continuum light sources have not resulted in limits of detection comparable with those for line sources in AA and AF, in theory at least they should be useful. In addition, the advantages of continuum light sources in AA and AF are that a single source suffices for essentially all elements; that continuum light sources are more stable, more reproducible from day to day, and longer lived; that multielement analysis would be instrumentally simple; that deviations of the shapes of analytical curves from growth curves are predictable from theory; and that spectral and flame parameters are easier to evaluate when continuum sources are used (see theory section). Continuum sources used in experimental studies have included primarily xenon arc lamps (150–900 watt) made by Osram and Hanovia.

D. Multielement Analysis

Without a doubt, multielement analysis is instrumentally simplest with AE. However, if a continuum source in AF were used only for those elements with resonance lines below about 3000 Å and AE for all elements with resonance lines above 3000 Å, the same multidetector spectrometric-measurement system could be used. Multielement analysis in AA is considerably more complex even if a continuum source is used because of the necessity of measuring a ratio of radiances (a transmittance or a fraction absorbed, an absorbance being even more complicated to measure because of the necessity of taking a logarithm) or a difference of radiances.

X. COMPARISON OF THEORETICAL PREDICTIONS AND EXPERIMENTAL RESULTS

A. The Radiance Expressions

The quantitative *radiance* expressions given in Section II are valid only under *rather idealized conditions,* as discussed below.

(i) Only a single, isolated spectral line in AA, AE, and AF is considered. This is a reasonable assumption for many elements studied in AA, AE, and AF using a good quality instrumental system. Actually, the radiance expressions can be extended to lines with fine structure and unresolved multiplots by using summation techniques described by Mitchell and Zemansky.[6]

(ii) The spectral line is broadened only by Doppler and collisional (Lorentz) effects. This is valid for most spectral lines in analytical flames.[4]

(iii) The flame has the same temperature at all points in the volume increment of importance at the height of observation. In Section IIA, the concept of thermodynamic equilibrium in flames was discussed. Flames are not adiabatic systems, because there are net transports of heat, radiation, and mass throughout the flame. However, if the rates of these transport processes are less than the rate at which energy is locally partitioned over the various degrees of freedom, then the concept of a local thermodynamic equilibrium characterized by a local temperature T has meaning for analytical flames. In flames produced using total-consumption nebulizer burners (unpremixed, diffusion turbulent flames) or using burners with chamber-type nebulizer burners (premixed laminar flames), there is considerable lateral and appreciable vertical temperature variation, and so the concept of a local flame temperature is applicable to only infinitesimal

* The workers at Imperial College, London (T.S. West, R.M. Dagnall, and co-workers) have had far greater success in preparing intense, stable, long-lived sources of most elements in the periodic table than have the workers at the University of Florida (J.D. Winefordner and co-workers).

flame volumes which make up the measured flame volume; the entire measured flame volume made up of many infinitesimal volumes all described by a different flame temperature can be characterized by an effective flame temperature for the entire volume. Laminar flames with an outer flame sheath[114] exhibit little lateral and vertical flame temperature variation and are more ideal for fundamental and possibly analytical studies.

In Section IIA, the equilibration of energy over the translational and internal degrees of freedom was discussed. Because flame temperatures measured[4] at short distances above the reaction zone are usually approximately the same as the equilibrium temperatures, the concentration of the major flame gas molecules (CO_2, CO, H_2O, and H_2) are close to their equilibrium values. The relative unimportance of ionization equilibria within the flame gases for excitation—de-excitation of analyte atoms was already discussed in Section IIA. Therefore, thermodynamic equilibrium with respect to the various degrees of freedom and the various flame equilibria is approximately valid; this is evident from temperature measurements based on a variety of different methods.[4]

(iv) The flame has the same atomic concentration at all points in the measured volume. Because of the variation of flame temperature and composition in the lateral and vertical positions of the measured volume of analytical flames without flame sheaths (see iii above), the free atom fraction β (and possibly the efficiency of producing an analyte ϵ) is also expected to vary from point to point, resulting again in an effective value of β (or effective value of ϵ) corresponding to the effective flame temperature and flame gas composition in the measured volume. Therefore, in most analytical flames the atomic concentration substituted into the radiance expressions is the effective concentration of atoms within the flame gases.

(v) In AA and AF, it was assumed that the flame cross section was rectangular (see Figure 2), whereas most analytical flames are generally rectangular only for AA, but circular for AF. For circular flames (cylindrical volume), the exact theoretical expressions are considerably more complicated. To allow a fair comparison of the radiance values in AA, AE, and AF, the same rectangular flame was assumed.

(vi) In AA and AF, the flame is uniformly illuminated. However, because of spatial inhomogeneity in the source radiance (particularly true of arc discharges), the radiant flux may not be uniform in the illuminated flame cell. Thus the number of radiationally excited analyte atoms within the flame gases may vary across the flame. This same trouble can arise from variation in atomic concentration within the flame gases (see item iv above).

(vii) In AF, the flame is excited by collimated light. If the flame is excited by means of a focused image (as is generally the case) and if the solid angle of radiation entering the flame is large, then light rays entering the flame at different angles will travel different distances through the flame and possibly through different flame gas compositions and temperatures. Thus different fractions of radiation will be absorbed for different rays. Similarly, if the measuring optics collect a large solid angle of radiation, the degree of self-absorption of the fluorescence radiation will vary depending upon the angle of the fluorescence being measured. Alkemade[1] states that as long as the maximum angle between different light rays is less than 30°, the deviation from the derived formulae is negligible.

(viii) In AF, the flame is uniformly illuminated [as in Figure 2-(3), not as in Figure 2-(4)] and the resulting atomic fluorescence over the entire flame surface at right angles to the excitation is measured [as in Figure 2-(3), not as in Figure 2-(5)]. In addition to the expected decrease in fluorescence resulting from incomplete illumination of the flame surface or incomplete measurement of the fluorescence (inner-filter effect), more subtle changes in the fluorescence radiance may result due to the variation of the atomic absorption coefficient with analyte concentration.

Invalidity of the above conditions can explain why the theoretical radiance expressions do not accurately describe the shapes of analytical curves observed in some experimental AA, AE, and AF studies. It should be recalled that the radiance expressions are only valid for the high- and low-optical-density asymptotes and

do not apply to the region near the intersection of these asymptotes where slopes considerably different from the extremes may result.[1,2] Experimental analytical curves do approach the shapes predicted by the radiance expressions discussed in Section III. However, many experimental analytical curves in AA, and especially in AF, tend to deviate considerably from the theoretically predicted curves, particularly at high analyte concentrations. Some of the reasons for these deviations have been discussed above in items i–viii. Because the authors of most experimental papers do not give sufficient information—particularly with regard to their source of excitation and their entrance optics—it is difficult to compare predicted and experimental values. A careful study by P.T.J. Zeegers[33] has shown excellent agreement between theoretically predicted and experimental analytical curves for Mg in a C_2H_2/air flame excited via both line (electrodeless discharge lamp) and continuum (900 watt xenon arc lamp) sources. Therefore, a careful investigation in which all experimental conditions and parameters are defined and known should allow prediction of radiance vs. atomic concentration curves. Any deviations of experimental analytical curves (signal vs. concentration of analyte nebulized into the flame) from the theoretical curves of radiance vs. atomic concentration of analyte must then result from factors that affect the linearity of the dependence of the atomic concentration of analyte in the flame on the concentration of analyte in the solution nebulized into the flame (see Section IV). For example, ionization at low analyte concentrations can cause an increase in slope in AA, AE, and AF, while incomplete solute vaporization, reduced sample transport rate, and reduced efficiency of aspiration at high analyte concentrations can all cause a decrease in slope.

Finally, from the analytical standpoint, the radiance expressions allow the analyst at least to anticipate certain behavior in analytical curves, e.g., the decrease in atomic fluorescence signals at high analyte concentrations when using narrow line sources. From the physical standpoint, analytical curves carefully prepared can be used to estimate the a-parameter and the fluorescence yield.

B. Comparison of Signal Strengths

The comparison of signal strengths in Section V also required rather idealized conditions which are listed below.

(i) The conditions and the validity of those conditions listed in part A of this section also apply here.

(ii) The same flame (as well as shape) type is used for AE, AA, and AF. It has already been stressed that different flames are probably ideal for AE, AA, and AF, although the C_2H_2/N_2O flame seems to be ideal for AE and AA and possibly for AF (see Section VIII).

(iii) The noise in each method is assumed to be the same. This assumption is shown to be invalid in Section VI.

(iv) The values of the parameters in Equations 39–42 are based on estimates from previous studies documented in the literature. It should be stressed that the radiance values of the line sources and the spectral radiance values of the continuum source are probably maximum values for those sources; some sources may not actually achieve those values because of improper tuning, losses of radiation due to window blackening, instability at powers needed, etc. If the source radiance or spectral radiance values are too large, this will produce a favorable effect upon AA and AF. It should also be stressed that the excitation solid angle (fraction is $\Omega_A/4\pi$) may have been too conservatively estimated for AF and this would have resulted in an unfavorable effect upon AF. The estimate of Y is probably too high for elements in the C_2H_2/N_2O flame and too low for elements in the $H_2/O_2/Ar$ flame. In the first case, the ratio of signals would favor AF unfairly and in the second case favor AE unfairly. It is also assumed that the same solid angle of measurement is collected by the spectrometric system for each method, whereas in many experimental systems larger solid angles will be collected in AE and AF than in AA. This assumption would then favor AA unfairly. All other values of parameters used to estimate the ratios probably do not favor any given method unfairly.

Of course, if different flames are used for the different flame methods, then it is necessary to account for the difference in ϵ, β, e_t, Q

and possibly F (assuming different burners and nebulizers are also used) for the different flames. The choice of flame type is probably the most critical factor in determining the actual radiance absorbed, emitted, or fluoresced in AA, AE, or AF, respectively.

As a result of the rather large number of approximations made to estimate the signal ratios, it is not too unexpected that poor correlation should be obtained between theoretical estimates of experimental signals listed in the literature. As a matter of fact, there has never been—to the knowledge of the authors of this manuscript—a careful study of the signal levels in AA, AE, and AF which would allow a good comparison of the theoretical and experimental signal ratios. Such a study would not be difficult and would be of real interest in determining usefulness of radiance expressions.

C. Comparison of Theoretical Limits of Detection

(i) The same conditions and the validity of these conditions and choice of parameter values listed in parts *A and B* of this section also apply here.

(ii) The estimates of noise for the three flame methods are very difficult to make and may certainly be suspected of being erroneous. The individual noises in the three methods are assumed to be independent. There is certainly some justification for this assumption.[34-36] The same good multiplier phototube is used for AA, AE, and AF. This is reasonable and relatively unimportant because shot noise does not contribute greatly to the total noise in any of the three methods. Flame background spectral radiances are estimated from our own experimental studies and should be reasonable for the three flames. The value of K in the signal expressions was estimated for a good analytical spectrometric system, including an 0.5-meter Ebert grating monochromator, the multiplier phototube described above, and an electronic measurement system with a frequency response bandwidth of 1 Hz. The flicker in the flame was also estimated from our own experimental studies on flames and seems reasonable. Perhaps the most uncertain value of all is the estimate of the flicker in the sources. We estimated the flicker factor ξ from our own studies, which have been very limited. However, estimates of flicker factors for sources (and flames) may be too conservative (too high).

A comparison of experimental and theoretical limits of detection has also never been carried out. Such a comparison is impossible unless all of the experimental conditions are accurately defined in the experimental measurements of limits of detection in AA, AE, and AF. Most experimental papers that give limits of detection do not give the flame-gas temperature and composition, and rarely give the spectral radiance and noise level of the flame and source and the characteristics of the current-measurement device. On the other hand, in theoretical papers on limits of detection a hypothetical instrumental system is assumed and no experimental results are given. Certainly, there is as yet too little experimental evidence to permit definitive evaluations of the theoretical predictions and the frequent apparent exceptions to them (apparent because there is really no way to correlate the theory and experiment because of the dearth of details given in the experimental papers). The experimental results in Table 4 and the conclusions in Section VII certainly seem to be consistent with the predictions involving the radiance (or signal) ratios in Table 3 and the noise ratios listed in Section VI. Again, a careful comparison of theoretical and experimental limits of detection (or ratios of limits of detection) would be of real interest in determining the analytical usefulness of the expressions presented in this manuscript.

XI. POSSIBLE FUTURE TRENDS IN AE, AA, AND AF

The authors expect great acceleration of research in the following areas during the next few years: (i) the use of continuum light sources in AF; (ii) the combination of AE and AF as a general analytical tool for trace metal analysis; (iii) the use of non-flame cells, such as graphite furnaces[124-133] in AA and AF; (iv) the use of pulsed light sources and detectors for AF; (v) the use of photon-counting techniques in AF, AE, and AA; (vi) the development of multielement analytical instrumentation using AE-AF.

REFERENCES

1. Alkemade, C.T.J., Talk at Sheffield Atomic Absorption Conference, Sheffield, England, July, 1969.
2. Hooymayers, H.P., *Spectrochim. Acta,* 23B, 567 (1968).
3. Zeegers, P.J.T., Smith, R., and Winefordner, J.D., *Anal. Chem.,* 40 (11), 26A (1968).
4. Alkemade, C.T.J. and Zeegers, P.J.T., Excitation and de-excitation in flames, in *Spectrochemical Methods of Analysis,* Winefordner, J.D., Ed., Interscience Publishers, New York, in press.
5. Alkemade, C.T.J., Proceedings of the X Colloquium Spectroscopicum Internationale, 1963, Lippincott, E.R. and Margoshes, M., Eds., Spartan Books, Washington, D.C., 1963, 143.
6. Mitchell, A.C.G. and Zemansky, M., *Resonance Radiation and Excited Atoms,* The University Press, Cambridge, 1961.
7. Unsöld, A., *Physik der Sternatmospheren,* Springer Verlag, Berlin, 1955.
8. Alkemade, C.T.J., Ph.D. Thesis, University of Utrecht, The Netherlands, 1954.
9. Hollander, T., Ph.D. Thesis, University of Utrecht, The Netherlands, 1954.
10. Van Trigt, C., Hollander, T., and Alkemade, C.T.J., *J. Quant. Spectrosc. Radiat. Transfer, 5,* 813 (1967).
11. de Galan, L., McGee, W.W., and Winefordner, J.D., *Anal. Chim. Acta,* 37, 436 (1967).
12. Alkemade, C.T.J., *Appl. Optics,* 7, 1261 (1968).
13. Young, C., *Tables for Calculating the Voigt Profile,* University of Michigan, Ann Arbor, 1965, ORA-05863, 1969.
14. Poesner, D.W., *Aust. J. Physics,* 12, 184 (1959).
15. Frish, S.E., Opticheskie Spektry Atomov, Gos. izdat. fiz-mat. lit., Moscow, 1963.
16. Hooymayers, H.P., Ph.D. Thesis, University of Utrecht, The Netherlands, 1966.
17. Winefordner, J.D., Parsons, M.L., Mansfield, J.M., and McCarthy, W.J., *Spectrochim. Acta,* 23B, 37 (1967).
18. Hooymayers, H.P., and Alkemade, C.T.J., *J. Quant. Spectrosc. Radiat. Transfer,* 6, 501 (1966).
19. Hooymayers, H.P. and Alkemade, C.T.J., *J. Quant. Spectrosc. Radiat. Transfer,* 6, 847 (1966).
20. Pearce, S.J., de Galan, L., and Winfordner, J.D., *Spectrochim. Acta,* 23B, 793 (1968).
21. Jenkins, D.R., *Spectrochim. Acta,* 23B, 167 (1967).
22. Jenkins, D.R., *Proc. Roy. Soc.,* A293, 493 (1966).
23. Hinnov, E., *J. Opt. Soc. Amer.,* 47, 151 (1967).
24. Hinnov, E. and Kohn, H., *J. Opt. Soc. Amer.,* 47, 156 (1967).
25. Winefordner, J.D., Vickers, T.J., and Remington, L.D., *Anal. Chem.* 37, 1216 (1965).
26. Vickers, T.J., Remington, L.D., and Winefordner, J.D., *Anal. Chim. Acta,* 36, 42 (1966).
27. Cowan, R.D. and Dieke, G.H., *Rev. Mod. Phys.,* 20, 418 (1948).
28. L'vov, B.V., *Zav. Lab.,* 28, 931 (1962).
29. Winefordner, J.D., *Record Chem. Progress,* 29, 25 (1968).
30. Rubeska, I., *Chem. Listy,* 59, 1119 (1965).

31. Rubeska, I. and Svoboda, V., *Anal. Chim. Acta,* 32, 253 (1965).

32. de Galan, L. and Winefordner, J.D., *Spectrochim. Acta,* 23B, 277 (1968).

33. Zeegers, P.J.T., unpublished data, University of Florida, Gainesville, 1968.

34. Winefordner, J.D. and Vickers, T.J., *Anal. Chem.,* 36, 1939 (1964).

35. Winefordner, J.D. and Vickers, T.J., *Anal. Chem.,* 36, 1947 (1964).

36. Mansfield, J.M., McCarthy, W.J., Winefordner, J.D., and Parsons, M.L., *Anal. Chem.,* 39, 439 (1967).

37. Winfordner, J.D. and Veillon, C., *Anal. Chem.,* 37, 416 (1965).

38. Winefordner, J.D., Mansfield, C.T., and Vickers, T.J., *Anal. Chem.,* 35, 1607 (1963).

39. de Galan, L. and Winefordner, J.D., *J. Quant. Spectrosc. Radiat. Transfer,* 7, 251 (1967).

40. Pungor, E., *Flame Photometry Theory,* Van Nostrand, New York, 1967.

41. Williams, F.A., 8th Symposium (International) On Combustion, Pasadena, Calif., 1960.

42. Williams, F.A., *Combustion Theory,* Addison-Wesley, Reading, Mass., 1965.

43. Fuchs, N.A., *Phys. Z. Sowjetunion,* 6, 224 (1934).

44. Okuyama, M. and Zung, J.T., *J. Chem. Phys.,* 46, 1580 (1967).

45. Zung, J.T., *J. Chem. Phys.,* 46, 2064 (1967).

46. Zung, J.T., private communication, University of Missouri, Columbia, 1968.

47. Frössling, N., *Gerlands Beitr. Geophys.,* 52, 170 (1938).

48. Mugele, R.A. and Evans, H.D., *Ind. Eng. Chem.,* 43, 1317 (1951).

49. Lapple, C.E., *Chem. Eng.,* 1 (May 20, 1960).

50. Herrmann, R. and Alkemade, C.T.J., *Flammenphotometrie,* 2nd ed., Springer, Berlin, 1960; *Chemical Analysis by Flame Photometry,* Gilbert, P.T., translator, John Wiley & Sons, New York, 1963.

51. Winefordner, J.D. and Latz, H.W., *Anal. Chem.,* 33, 1727 (1961).

52. Snelleman, W., Ph.D. Thesis, University of Utrecht, The Netherlands, 1965.

53. van der Held, E.T.M., Ph.D. Thesis, University of Utrecht, The Netherlands, 1932.

54. Fassel, V.A. and Becker, D.A., in Proceedings of XIII Colloquium Spectroscopium Internationale, Ottawa, Adam Hilger, London, 1968, 269.

55. Fassel, V.A. and Becker, D.A., *Anal. Chem.,* 41, 1522 (1969).

56. Cowley, T.G., Fassel, V.A., and Kniseley, R.N., *Spectrochim. Acta,* 23B, 771 (1968).

57. Koirtyohann, S.R. and Pickett, E.E., Talk at XI Colloquium Spectroscopicum Internationale, Ottawa, Canada, 1967.

58. de Galan, L., Talk at Sheffield Atomic Absorption Conference, Sheffield, England, July, 1969.

59. Prugger, H., *Spectrochim. Acta,* 24B, 197 (1969).

60. Klein, L., *Appl. Optics,* 7, 677 (1968).

61. Mansfield, J.M., Bratzel, M.P., Norgordon, H.O., Knapp, D.O., Zacha, K.E., and Winefordner, J.D., *Spectrochim. Acta,* 23B, 389 (1968).

62. Pivonsky, M. and Nagel, M.R., *Tables of Black Body Radiation Functions,* Macmillan Co., New York, 1961.

63. Parsons, M.L., McCarthy, W.J., and Winefordner, J.D., *Appl. Spectrosc.*, 20, 223 (1966).

64. Bair, E.J., *Introduction to Chemical Analysis*, McGraw-Hill, New York, 1962.

65. L'vov, B.V., Atomno-absorbtsionnyj spektratnyj analiz, Izdatelstvo "Nauka," Moscow, 1966.

66. Kahn, H., Trace inorganics in water, in *Advances In Chemistry*, Series No. 73, American Chemical Society, Washington, D.C., 1968.

67. Zacha, K.E., Bratzel, M.P., Winefordner, J.D., and Mansfield, J.M., *Anal. Chem.*, 40, 1733 (1968).

68. Pickett, E.E. and Koirtyohann, S.R., *Spectrochim. Acta*, 23B, 235 (1968).

69. Dagnall, R.M., Taylor, M.R.G., and West, T.S., *Spectrosc. Lett.*, 1, 397 (1968).

70. Pickett, E.E. and Koirtyohann, S.R., *Spectrochim. Acta*, 24B, 325 (1969).

71. Dagnall, R.M., Taylor, M.R.G., and West, T.S., *Spectrosc. Lett.*, in press.

72. Fassel, V.A. and Golightly, D.W., *Anal. Chem.*, 39, 466 (1967).

73. Manning, D.C. and Heneage, P., *Atomic Absorption Newsletter*, 7, 80 (1968).

74. Hingle, D.N., Kirkbright, G.F., and West, T.S., *Analyst*, 93, 522 (1968).

75. Bratzel, M.P., Dagnall, R.M., and Winefordner, J.D., University of Florida, Gainesville, unpublished results, April 1969.

76. Dagnall, R.M., Thompson, K.C., and West, T.S., *Talanta*, 14, 1467 (1967).

77. Hobbs, R.S., Kirkbright, G.F., and West, T.S., *Analyst*, 94, 554 (1969).

78. Matousek, J. and Sychra, V., *Anal. Chem.*, 41, 518 (1969).

79. Mansfield, J.M., Winefordner, J.D., and Veillon, C., *Anal. Chem.* 37, 1049 (1965).

80. Vickers, T.J. and Merrick, S.P., *Talanta*, 15, 873 (1968).

81. West, T.S. and Williams, X.K., *Anal. Chim. Acta*, 42, 29 (1968).

82. Dagnall, R.M., Thompson, K.C., and West, T.S., *Talanta*, 14, 1151 (1967).

83. Cresser, M.S. and West, T.S., *Spectrosc. Lett.*, 2, 9 (1969).

84. Browner, R.F., Dagnall, R.M., and West, T.S., Imperial College, London, England, unpublished work, April 1969.

85. Dagnall, R.M., Thompson, K.C., and West, T.S., *Talanta*, 14, 557 (1967).

86. Kniseley, R.N., Butler, C.C., and Fassel, V.A., *Anal. Chem.*, 41, 1494 (1969).

87. Kirkbright, G.F., Sargent, M., and West, T.S., *Talanta*, 16, 245 (1969).

88. Fassel, V.A., Mossotti, V.G., Grossman, W.E.L., and Kniseley, R.N., *Spectrochim. Acta*, 22, 347 (1966).

89. Ellis, D.W. and Demers, D.R., Talk given at Miami Beach ACS Meeting, April 1967.

90. Veillon, C., Mansfield, J.M., Parsons, M.L., and Winefordner, J.D., *Anal. Chem.*, 38, 204 (1966).

91. Ellis, D.W. and Demers, D.R., *Anal. Chem.*, 38, 1943 (1966).

92. Ivanov, N.P. and Kazireva, N.A., *Zh. Analit. Khim.*, 19, 1266 (1966).

93. Pickett, E.E., and Koirtyohann, S.R., *Spectrochim. Acta*, 23B, 673 (1968).

94. Robinson, J.W. and Hsu, C.J., *Anal. Chim. Acta*, 43, 109 (1968).

95. Bratzel, M.P., Dagnall, R.M., and Winefordner, J.D., *Anal. Chem.*, 41, 1527 (1969).

96. Fassel, V.A., Rasmuson, J.O., and Cowley, T.G., *Spectrochim. Acta*, 23B, 579 (1968).

97. Yasuda, K., *Anal. Chem.*, 38, 592 (1966).

98. Rann, C.S., *Spectrochim. Acta*, 23B, 827 (1968).

99. Winefordner, J.D. and Vickers, T.J., *Anal. Chem.*, 36, 161 (1964).

100. de Galan, L. and Winefordner, J.D., *Anal. Chem.*, 38, 1412 (1966).

101. Koirtyohann, S.R. and Pickett, E. E., *Anal. Chem.*, 37, 601 (1965).

102. Willis, J.B., Atomic absorption spectroscopy, in *Methods of Biochemical Analysis*, Glick, D., Ed., Interscience Publishers, New York, 1963.

103. Koirtyohann, S.R. and Pickett, E.E., *Anal. Chem.*, 38, 1087 (1966).

104. Kahn, H.L., *Atomic Absorption Newsletter*, 7, 40 (1968).

105. Fiorino, J., Ph.D. Thesis, Iowa State University, Ames, 1969.

106. Slavin, W., *Atomic Absorption Spectroscopy*, Interscience Publishers, New York, 1968.

107. Bratzel, M.P., Dagnall, R.M., and Winefordner, J.D., *Anal. Chem.*, 41, 713 (1969).

108. Smith, R., Atomic flame fluorescence, in *Spectrochemical Methods of Analysis*, Winefordner, J.D., Ed., Interscience Publishers, New York, in press.

109. Elwell, W.T. and Gidley, J.A.F., *Atomic Absorption Spectrophotometry*, Macmillan, New York, 1962.

110. Robinson, J.W., *Atomic Absorption Spectroscopy*, Dekker, New York, 1968.

111. Ramírez-Muñoz, J., *Atomic Absorption Spectroscopy*, Elsevier, New York, 1968.

112. Mavrodineanu, R. and Boiteux, H., *Flame Spectroscopy*, John Wiley & Sons, New York, 1965.

113. Dean, J., *Flame Photometry*, McGraw-Hill, New York, 1960.

114. Zeegers, P.J.T., Ph.D. Thesis, The University of Utrecht, The Netherlands, 1966.

115. Gilbert, P.T., Symposium on Spectroscopy, *Amer. Soc. Testing Materials, Spec. Tech. Publ.*, 269, 1960.

116. Bowman, J. and Walsh, A., *Spectrochim. Acta*, 22, 205 (1966).

117. Sullivan, J.V. and Walsh, A., *Spectrochim. Acta*, 21, 721 (1965).

118. Armentrout, D.N., *Anal. Chem.*, 38, 1235 (1966).

119. Dinnin, J.I., *Anal. Chem.*, 39, 1491 (1967).

120. West, T.S. and Williams, X.K., *Anal. Chem.*, 40, 335 (1968).

121. Dagnall, R.M., Thompson, K.C., and West, T.S., *Talanta*, 14, 551 (1967).

122. Dagnall, R.M., Přibil, R., and West, T.S., *Analyst*, 93, 281 (1968).

123. Marshall, G.B. and West, T.S., *Talanta*, 14, 823 (1967).

124. L'vov, B.V., *Spectrochim. Acta*, 17, 761 (1961).

125. L'vov, B.V., I.U.P.A.C. XXth Congress, Moscow, U.S.S.R., July 1965.

126. L'vov, B.V., *J. Appl. Spectrosc.*, 8, 517 (1968).

127. Massmann, H., *Z. Anal. Chem.*, 225, 203 (1967).

128. Woodriff, R., Stone, R.W., and Held, A.M., *Appl. Spectrosc.*, 22, 408 (1968).

129. Woodriff, R. and Stone, R.W., *Appl. Optics*, 7, 1337 (1968).

130. Massmann, H., *Spectrochim. Acta*, 23B, 215 (1968).

131. West, T.S. and Williams, X.K., *Anal. Chim. Acta*, 45, 27 (1969).

132. Bratzel, M.P., Dagnall, R.M., and Winefordner, J.D., Mid-American Symposium on Spectroscopy, Chicago, May 1969.

133. Winefordner, J.D., Talk at Sheffield Atomic Absorption Conference, Sheffield, England, July 1969.

APPENDIX

Definitions and Units of Symbols Used in Paper

A_t = total absorption, cm or nm

$A_t(nL)$ = total absorption for a concentration-path length product of nL, cm or nm

A_{u0} = Einstein coefficient of spontaneous emission, sec^{-1}

AA = Atomic Absorption Flame Spectrometry

AAC = Atomic Absorption Flame Spectrometry with a Continuum Source

AAL = Atomic Absorption Flame Spectrometry with a Line Source

AE = Atomic Emission Flame Spectrometry

AF = Atomic Fluorescence Flame Spectrometry

AFC = Atomic Fluorescence Flame Spectrometry with a Continuum Source

AFL = Atomic Fluorescence Flame Spectrometry with a Line Source

a = the a-parameter, $\sqrt{\ln 2}\ (\Delta\lambda_C/\Delta\lambda_D)$, dimensionless

B = radiance, erg $sec^{-1}cm^{-2}ster^{-1}$

B_{AA} = radiance of atomic absorption, erg $sec^{-1}cm^{-2}ster^{-1}$

B_{AAC} = radiance of atomic absorption using a continuum source, erg $sec^{-1}cm^{-2}ster^{-1}$

B_{AAL} = radiance of atomic absorption using a line source, erg $sec^{-1}cm^{-2}ster^{-1}$

B_{AE} = radiance of atomic emission, erg $sec^{-1}cm^{-2}ster^{-1}$

B_{AF} = radiance of atomic fluorescence, erg $sec^{-1}cm^{-2}ster^{-1}$

B_{AFC} = radiance of atomic fluorescence produced using a continuum source, erg $sec^{-1}cm^{-2}ster^{-1}$

B_{AFL} = radiance of atomic fluorescence produced using a line source, erg $sec^{-1}cm^{-2}ster^{-1}$

$B_{A\lambda}$ = spectral radiance absorbed at wavelength λ, erg $sec^{-1}cm^{-2}ster^{-1}nm^{-1}$ (or cm^{-1})

$B_{B\lambda}$ = spectral radiance of black-body at wavelength λ, erg $sec^{-1}cm^{-2}ster^{-1}nm^{-1}$ (or cm^{-1})

$B_{B\lambda_0}$ = spectral radiance of a black-body at wavelength λ_0, erg $sec^{-1}cm^{-2}ster^{-1}nm^{-1}$ (or cm^{-1})

$B_{C\lambda}$ = spectral radiance absorbed at wavelength λ, erg $sec^{-1}cm^{-2}ster^{-1}nm^{-1}$ (or cm^{-1})

$B_{C\lambda_0}$ = spectral radiance of continuum source at wavelength λ_0, erg $sec^{-1}cm^{-2}ster^{-1}nm^{-1}$ (or cm^{-1})

B_L = radiance of line source, erg $sec^{-1}cm^{-2}ster^{-1}$

$B_{L\lambda}$ = spectral radiance of line source at wavelength λ, erg $sec^{-1}cm^{-2}ster^{-1}nm^{-1}$ (or cm^{-1})

BM = effective gain of multiplier phototube, dimensionless

$B_{S\lambda}$ = spectral radiance of source at wavelength λ, erg $sec^{-1}cm^{-2}ster^{-1}nm^{-1}$ (or cm^{-1})

$B(T)$ = normalized electronic partition function of atom, dimensionless

B_λ = spectral radiance of any radiating body at wavelength λ, erg $sec^{-1}cm^{-2}$ $ster^{-1}nm^{-1}$ (or cm^{-1})

C = solution concentration of analtye, moles cm^{-3}

c = speed of light *in vacuo*, cm sec^{-1}

$c_1 = 8\pi hc^2\lambda_0^{-5}$, erg $sec^{-1}cm^{-2}ster^{-1}nm^{-1}$

$c_2 = \sqrt{\pi}/2\sqrt{\ln 2}$, dimensionless

$c_3 = \sqrt{\pi}/\sqrt{\ln 2}$, dimensionless

dE_k = spread of kinetic energy, erg

E_i = energy of electronic level i, erg

E_k = kinetic energy, erg

E_u = energy of electronic level u, erg

e = charge of electron, esu or coulomb

e_f = flame gas expansion factor, dimensionless

e_λ = emissivity per cm of radiating layer, cm^{-1}

F = solution transport rate as determined by nebulizer, cm^3 sec^{-1}

f_{0u} = absorption oscillator strength, dimensionless

$f(E_k)$ = fraction of particles with mass m and kinetic energy E_k, dimensionless

f_1 = low cut-off frequency of measurement system, Hz

G_S = ratio of signal in AAC, AAL, AFC, or AFL to that in AE, dimensionless

g_j = statistical weight of level j, dimensionless

h = Planck constant, erg sec^{-1}

K = instrumental constant, ampere cm^2ster erg^{-1} sec

$K_d(T)$ = dissociation energy of diatomic molecule as function of temperature, cm^{-3}

$K_i(T)$ = ionization energy of atom as a function of temperature, cm^{-3}

k = Boltzmann constant, erg $°K^{-1}$

k_o = atomic absorption coefficient for pure Doppler broadening defined at λ_o, cm^{-1}

k_m = maximum atomic absorption coefficient at the absorption line peak, λ_o, cm^{-1}

k_{X_i} = second order rate constant for deactivation of analyte atoms via collisions with X_i, cm^3sec^{-1}

k_λ = atomic absorption coefficient at wavelength, cm^{-1}

L = path length (see Figure 2), cm

l = path length (see Figure 2), cm

l' = height of flame cell (see Figure 2), cm

M = molecular weight of emitting or absorbing atom, g

m = mass electron

N_{AE} = total noise current at photodetector output in AE (or AA or AF), amperes

N_t = total noise current at photodetector output, amperes

N_{flame} = flame fluctuation noise current at photodetector output, amperes

N_{shot} = shot noise current at photodetector output, amperes

N_{source} = source fluctuation noise current at photodetector output, amperes

n = concentration of atom in ground state, number of ground state species, cm^{-3}

n_A = concentration of species A, number of species A cm^{-3}

n_e = total concentration of electrons in flame, number of electrons cm^{-3}

n_f = free electron concentration of flames, number of free electrons cm^{-3}

n_T = total concentration of analyte atoms in all forms, number of analyte atoms cm^{-3}

n_t = total concentration of atoms in all electronic levels, number of atoms in all electronic state cm^{-3}

n_u = concentration of atoms in level u, number of atoms in level u cm^{-3}

Q = flow rate of unburnt gases into flame, $cm^{-3}sec^{-1}$

S = photodetector signal, amperes

s = spectral bandwidth of monochromator, nm

T = temperature of gas, °K

T_F = temperature of flame, °K

T_S = effective temperature of source, °K

V_d = dissociation energy of monoxide, erg

$v = 2\sqrt{\ln 2}\,(\lambda - \lambda_0)/\Delta\lambda_D$, dimensionless

Y = quantum yield for resonance absorption—resonance fluorescence, quanta emitted per quanta absorbed, dimensionless

y = integration variable for Voigt profile defined in Equation 9

$Z = 6.62 \times 10^{15}\, g_o/\lambda_o^2 g_u$, dimensionless

α_λ = absorption factor, dimensionless

α_{AAC} = fraction of radiation absorbed when using a continuum source in atomic absorption, dimensionless

α_{AAL} = fraction of radiation absorbed when using a line source in atomic absorption, dimensionless

β = free-atom fraction, dimensionless

γ = photoanodic sensitivity of multiplier phototube, amperes at photoanode per watt radiant power on photocathode

Δf = frequency response bandwidth of measurement electronics, Hz

ΔL = path length interval (see Figure 2), cm

Δl = path length interval (see Figure 2), cm

$\Delta\lambda_A$ = absorption line halfwidth, cm (or nm)

$\Delta\lambda_D$ = Doppler halfwidth of resonance line, cm (or nm)

$\Delta\lambda_S$ = source line halfwidth, cm (or nm)

$\Delta\lambda_L$ = Lorentzian halfwidth of resonance line, cm (or nm)

$\delta_o = k_o/\kappa_o nf$, given by Voigt profile integral in Equation 5 for a given a-parameter and a wavelength of $\lambda = \lambda_o$, dimensionless

ϵ = aspiration efficiency, dimensionless

ϵ_λ = emissivity of radiating body, dimensionless

ζ = fraction that rms flicker current is of total signal upon which flicker is superimposed, dimensionless

θ_f = area of fluorescence emission in direction of monochromator, cm²

θ_s = area of image of source of excitation upon entrance slit of monochromator, cm²

$\kappa_o' = k_o/nf$, a modified atomic absorption coefficient, cm²

λ_o = wavelength of line center, cm

$\pi = 3.1416 \ldots$, dimensionless

Ω = solid angle of radiation collected by monochromator, ster

Ω_λ = solid angle of radiation collected from source by entrance optics in atomic fluorescence, ster